SURFACE FUNCTIONALIZATION OF POLYMER SUBSTRATES AND NANOPARTICLES VIA PULSED PLASMA POLYMERIZATION PROCESS

by

JING WU

Presented to the Faculty of the Graduate School of

The University of Texas at Arlington in Partial Fulfillment

of the Requirements

for the Degree of

MASTER OF SCIENCE IN CHEMISTRY

THE UNIVERSITY OF TEXAS AT ARLINGTON

August 2005

ACKNOWLEDGEMENTS

I would like to express my deep gratitude to my research advisor Professor Richard B. Timmons for his encouragement, guidance and support throughout the course of this work.

I would also like to thank Professor Zoltan A. Schelly and H. V. Rasika Dias for their service on my supervising committee. I particularly owe many thanks to Dr. Charles R. Savage and Dr. Qian Qiu Zhao (Dupont CR&D) for their sincere advice and assistance throughout my graduate study and internship. Additionally, I wish to acknowledge Dr. Samuel Sanchez, Jayhun Cho for their valuable assistance, collaboration and valuable discussions.

My special thanks go to my husband Chenglin Chi for his love and support, and my parents and brother for their encouragement and understanding.

June 4, 2005

ABSTRACT

SURFACE FUNCTIONALIZATION OF POLYMER SUBSTRATES AND NANOPARTICLES VIA PULSED PLASMA POLYMERIZATION PROCESS

Publication No._____

Jing Wu

The University of Texas at Arlington, 2005

Supervising Professor: Richard B. Timmons

This thesis investigates the RF plasma polymerizations of chlorinated saturated linear monomer 1,1,1-trichloroethane and the dicarboxylic citraconic acid. It utilizes a variable duty cycle plasma technique to provide film chemistry control during the plasma polymerization process. Film chemical compositions and deposition rates were characterized as functions of the plasma processing conditions. In each system studied, spectroscopic analyses revealed that large progressive changes in film compositions were obtained with sequential variations in plasma duty cycles in the plasma polymerization of

both 1,1,1-trichloroethane and citraconic acid.

The plasma approach was also employed to modify the surfaces of nanoparticles. Thin polymeric films, produced from allylamine monomer, were pulsed plasma polymerized onto surfaces of 35nm (average particle size) gamma iron oxide nanoparticles. The morphology, structure and composition of the allylamine coated gamma iron oxide nanoparticles were characterized using a variety of analytical techniques. High resolution transmission electron microscope measurements revealed an ultra thin film of allylamine (4 nm) was uniformly deposited on surfaces of gamma iron oxide nanoparticles by the pulsed plasma polymerization process. Fourier transform infrared, X-ray photoelectron spectroscopy and time-of-flight secondary ion mass spectroscopy measurements all confirmed the allylamine deposition and existence of free amine groups on gamma iron oxide nanoparticle surfaces. The free amine groups of polyallylamine provide sites for immobilization of foreign molecules, suggesting that the allylamine coated gamma iron oxide nanoparticles can be employed to deliver drugs to targeted tissues and organs using magnetic focusing techniques.

TABLE OF CONTENTS

LIST OF ILLUSTRATIONS

LIST OF TABLES

CHAPTER 1

INTRODUCTION

1.1 Pulsed Plasma Polymerization Process

Plasma is a partially ionized gaseous complex composed of electrons, free radicals, ions, photons and a great number of neutral molecules in both ground and excited states. [1] In a plasma, gas molecules undergo dissociation and excitation followed by their reverse processes, recombination and relaxation. Dissociation and excitation cause intra-molecular bond cleavages in a molecule and/or promote a bound electron to a higher energy state, respectively, as a result of inelastic collisions with more energetic species. A variety of reactive radical species are generated via bond scission and excitation during the fragmentation of a monomer molecule. [2]

Plasma polymerization processes involve recombination of various molecular fragments at free radical sites, whose generation depends on the chemical structure of the monomer and the plasma operating conditions. Polymerization (deposition) and ablation (etching) occur simultaneously. The competitive balance of these two processes is dependent on the nature of the starting monomer and energy input level.

Pulsed plasma polymerization employs variable duty cycles (on/off time) instead of CW (continuous wavelength) to obtain enhanced film chemistry controllability during plasma coating processes. In this approach, the plasma "ON" period produces a burst of reactive species, which are then permitted to undergo radical decay processes during the

plasma "OFF" relaxation periods. During these off times, the radicals react with fresh monomer molecules, presumably via a more conventional radical polymerization pathway, so that a more ordered and selective chemistry occurs during plasma off times. Since the power is turned off during major portions of the polymerization process, the average power employed under pulsed conditions is significantly lower than those attainable under CW conditions. [3] This average power input is calculated from the equation:

$$P_{ave} = \left(\frac{t_{on}}{t_{on} + t_{off}}\right) P_{peak}$$

where t_{on} and t_{off} are the plasma on and off times. Overall, the pulsed plasma technique is more conductive to the retention of monomer functionalities than is obtainable under CW conditions.

The properties of plasma polymers are determined by plasma polymerization conditions and the monomer employed. Under the variable duty cycle pulsed plasma technique, applied power, duty cycle (on/off times), reaction pressure and monomer flow rate are the variables employed to control plasma phase reactions. Plasma polymers are also highly dependent upon the reactor characteristics (reactor geometry, electric power mode, size and distance between electrodes) and other factors such as sample positions relative to the plasma zone and substrate temperature.

Overall, the pulsed plasma polymerization process is a relatively simple, solvent-less, one step procedure for film deposition. The coating technique causes minimal alteration to the bulk properties of the substrate, as the extent of modification is usually restricted to the outmost layer.[1] Also, unusually wide ranges of monomers are available

for use, in many cases providing polymer films of unique composition. Also, of major consideration is the fact that it is possible to attain rather exact control of film thickness using plasma polymerization.

1.2 Ultra Thin Films for Use in Solventless Adhesives as Generated by Pulsed Plasma Polymerization

The 1st part of this thesis describes studies evaluating the use of plasma polymerizations for production of ultra-thin adhesive films. It is anticipated that a variety of uses will be identified for this new technology. Of special interest are applications in the area of micro-fluidics where film thickness control is of paramount important. The adhesive films are to be synthesized using a variable duty cycle pulsed plasma technique to generate films of the requisite compositions.

Micro-fluidic systems are used extensively at present, for example, in the area of biotechnology. They are employed in analysis of DNA and protein, [4] sorting of cells, [5] high through put screening, [6] chemical reactions, [7] and transfers of small volumes (1 to 100 μls) of materials. [8] These micro-fluidic devices have dimensions ranging from millimeters down to micrometers. A key factor in their fabrication is the creation of tiny hemi-spherical shaped canals. Sandia National Laboratory has developed and patented a technique for obtaining a series of hollow tunnels (8-100 μm in diameter) through which micro fluids can move on the surface of silicon chips. [9] However, it is also of interest to develop polymer-based systems for use in this area. Use of polymeric substrates, in place of silicon, requires development of ultra-thin adhesives to avoid damaging pre-trenched materials when assembling substrates having micro-size channels. A particularly challenging aspect is that these devices will be typically subjected to very large pressure

to distribute liquids, as required in moving liquids through such narrow channels. The plasma polymerization technique offers a potentially useful approach in fabricating ultra-thin adhesive layers for subsequent use as adhesives.

Adhesive bonding is a process in which two substrates are solidly and permanently bonded using an adhesive. The following parameters have been found to affect joint durability: [10](1) characteristics of the materials to be joined, (2) surface pretreatment, (3) type of adhesive and its handling, (4) curing of the adhesive, (5) applied stress and environmental performance requirements of the adhesive bonded. A wide variety of materials have been employed as adhesives. Generally, these materials involve pastes and / or liquids in which polymerization processes are involved in creating the adhesive bonds.

There have been a number of prior studies involving adhesive studies employing plasma discharge techniques. The vast majority of these studies have centered on attempts to achieve adhesion of metal films to polymer substrates. In general, non-polymerizable gases (e.g. Ar, O_2, etc.) were employed to activate a polymeric surface for subsequent bonding of the metal film. The metal films are deposited on the plasma-activated surfaces using evaporation or sputtering techniques. Examples of such work involve studies with O_2, Ar, air, N_2, H_2 and NH_3 as plasma discharge gases. [11-19] The gas discharges employed increased the wettability and interfacial energy of the polymeric surfaces. More recently, the plasma approach has been employed to deposit polymeric thin films for subsequent use as adhesives. Work in this area has included plasma polymerizations of glycidyl methacrylate [20a] and poly (2-hydroxyethyl methacrylate) [21]. These studies of Badyal and co-workers involved use of pulsed plasma polymerization to

introduce epoxide-containing films on both substrate surfaces. These materials were subsequently bonded via use of a thin liquid film of ethylenediamine, applied to each surface, followed by oven curing.

Chapter 3.1 presents a study to develop a solventless ultra-thin film process to bond polymeric poly (ether ether ketone) (PEEK) substrates. It involves systematic studies of experimental variables to optimize adhesive properties of these films, consistent with maintaining minimal film thickness. The pulsed plasma approach is employed to synthesize thin films containing reactive functional groups. The basic idea is to deposit different functional groups on each substrate and subsequently bond the substrates via simple covalent bond formation between the two plasma deposited films. For example, if film A contains epoxide groups and film B contains amine groups, it should be possible to react these two films via formation of secondary alcohol bonds between these two reactive groups, as shown below.

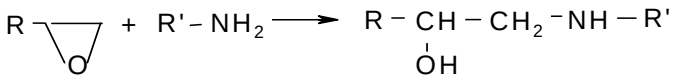

The pulsed plasma technique is employed as it has been shown, using unsaturated functionalized monomers, that it is possible to conserve relatively high percentages of the reactive functional groups in the polymeric films when low duty cycle (low average power input) conditions are employed. [22] The reactive groups investigated in the present study include anhydride, epoxide, and amine groups.

1.3 Plasma Polymerization of Di-carboxylic Acid

Surface modifications to introduce carboxylic acid groups have become increasingly important to improve adhesion and interfacial shear strength of carbon fibers

with epoxy resin matrix through covalent bonding, [23] to enhance permselectivity of ultra-filtration membranes due to its negatively charged surface, [24] and to act as reactive or anchor sites for further derivative reactions, such as the covalent immobilization of proteins or enzymes. [25]

Two plasma processes have been used for the introduction of carboxylic groups onto a polymer surface: (1) a surface is exposed to the plasma of a non-polymerizable gas such CO_2; [26] (2) the plasma polymerization of a carboxylic group containing organic monomer, such as acrylic acid, to form a plasma polymer on a surface. [25] [27] With the first process it is difficult to obtain a rich carboxylic specific surface because a mixture of O-containing functionalities was deposited resulting in a surface which contains only a limited amount of carboxylic groups. So the second process is the more commonly used approach. However, with the second process, the fragmentation of the monomers within the plasma discharge zone favors elimination of H_2O, CO, CO_2 and other oxygen containing products, leading to a cross-linked hydrocarbon polymer. In order to achieve high retention of carboxylic groups in the plasma polymers, strategies such as employing a low power input or pulsed plasma mode was applied. In this work, a new attempt, a starting monomer containing two carboxylic groups, was made to obtain high retention of carboxylic acid. This work presents the first reported study of the pulsed plasma polymerization of citraconic acid.

1.4 Amine Groups ($-NH_2$) Functionalized γ-Fe_2O_3 Nanoparticles by Pulsed Plasma Polymerization Process

Superparamagnetic iron oxide nanoparticles are being employed in a wide range of biomedical applications including use as MRI (magnetic resonance imaging)

diagnostic contrast reagents [28-31], separation of cells, bio-organisms and proteins [32][38], hyperthermia tumor treatment [33] and site-specific drug delivery [34-37]. Superparamagnetic iron oxide nanoparticles, like magnetite (Fe_3O_4) and maghemite (γ-Fe_2O_3) exhibit multifunctional properties, such as small size, extremely high surface area, low toxicity and superparamagnetism in which particles do not remain magnetized until exposure to an external magnetic field. [39,40]

Most of these biomedical applications of superparamagnetic nanoparticles require nanoparticles to be durable and biocompatible in biological environments. Functionalization and surface modification of nanoparticles have been applied to improve its durability, biocompatibility, and immobilization of foreign molecules as well. [38,41,42] Amine ($-NH_2$) groups have been used for DNA extraction process [43,44] and immobilization of BSA [42] via covalent bonding by liquid phase reaction. In this work, the pulsed plasma polymerization technique is employed to introduce amine ($-NH_2$) groups to surfaces of γ-Fe_2O_3 nanoparticles.

CHAPTER 2

EXPERIMENTAL

2.1 Pulsed Plasma Polymerization System and Operation Procedures

Pulsed plasma thin film depositions were carried out in three different systems. All three reactors had essentially identical electronic systems, pressure controls and monitoring system, but different shapes of reactors. The electronic system included a function generator (Wavetek modle 166), pulse generator (Tetronix model 2101), RF amplifier (ENI modle A 150), frequency counter (HP model 5381A), wattmeter (Bird) and a homemade capacitor/inductor matching network. An oscilloscope was used to verify plasma pulse widths, peak power inputs and minimization of reflected power during the RF pulsed operation. All experiments were carried out at 13.56 MHz. Pressure inside the reactor was monitored by an exhaust valve controller (model 252) and controlled using a butterfly valve (MKS Baratron model 252A) connected in a feedback loop with a pressure transducer. The reactor system was connected to a rotary vane vacuum pump, via a liquid N_2 cold trap, to prevent contamination of the reaction chamber by back streaming of vacuum pump oil vapor and contamination of the vacuum pump by condensable organic vapors.

System one had a 30.5 cm long and 10 cm inside diameter cylindrical Pyrex glass tubular reactor. Two external concentric metal rings located at the ends of the reactor vessel provided radio frequency power to the reactor. The electrode spacing was 15cm.

The ground electrode was located at the downstream position. Samples were placed on the top of a piece of glass located at the center of reaction chamber. Plasma polymerization of glycidyl methacrylate and ethylenediamine were done in this reactor. Fig 2.1 shows the pulsed plasma reactor and its associated electronics.

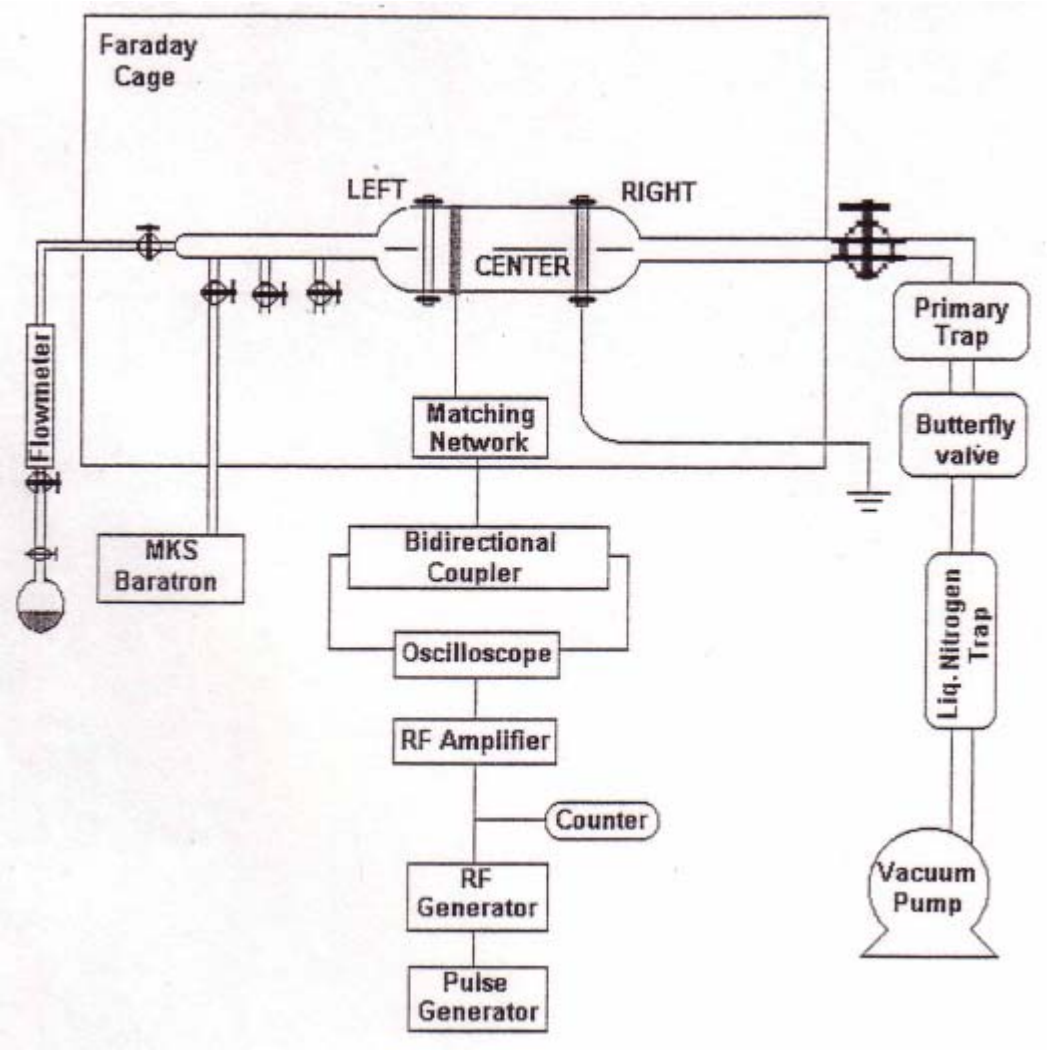

Fig. 2.1 Schematic diagram of the pulsed RF plasma reactor using a Cylindrical Pyrex Glass

System two was usually employed for the surface functionalization of powders. It had a 45 cm long and 5 cm inside diameter cylindrical Pyrex glass reactor. The external concentric metal rings located at the ends of the reactor vessel provided radio frequency

power to the reactor. The electrode spacing was 20 cm. At the ends of the Pyrex glass reactor, there were 360 degree rotating ferro-fluidic valves which permitted continuous rotation of the reactor during powder coating. The rotation of the reactor provided continuous mixing and agitation of the powders thus providing more uniform surface coatings. The amination of γ-Fe_2O_3 nanoparticles were carried out in this system. Fig. 2.2 shows the apparatus of rotating system.

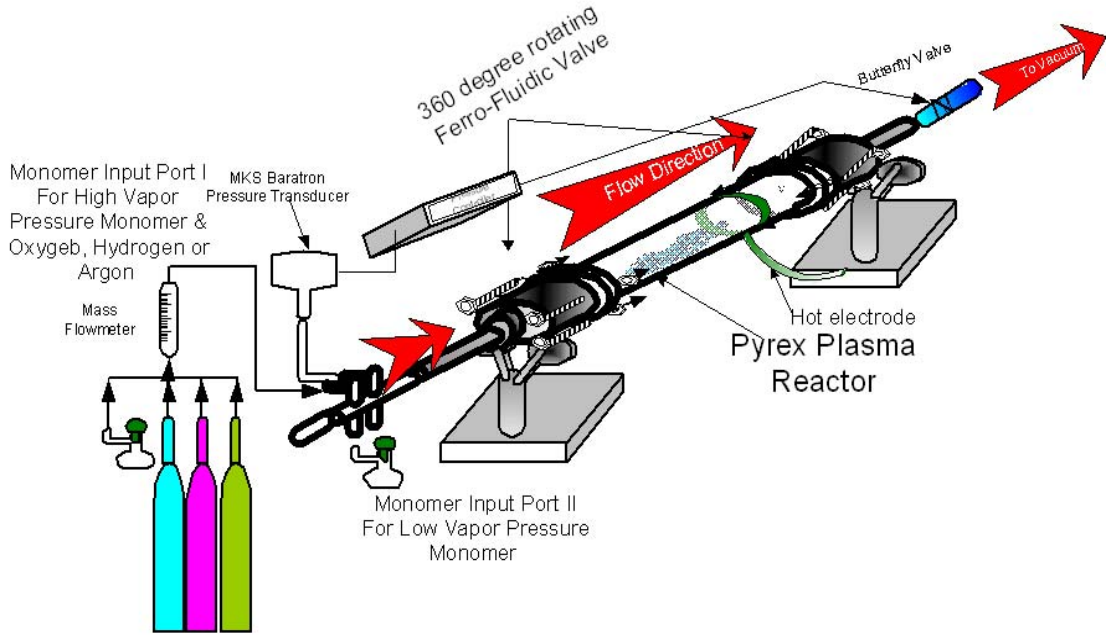

Fig. 2.2 Schematic diagram of the pulsed RF plasma reactor using a rotating Cylindrical Pyrex Glass

System three was a high temperature plasma polymerization system, which permitted use of less volatile monomers. Additionally, the effect of substrate temperature on the plasma polymerization can be evaluated. The main difference between this system and the other two was the reactor geometry. The main plasma chamber reactor employed in this system was a bell shaped Pyrex glass. It was observed that this reactor

significantly improves film thickness uniformity, especially when dealing with larger substrates. Fig 2.3 is the schematic diagram of the heatable plasma reactor system.

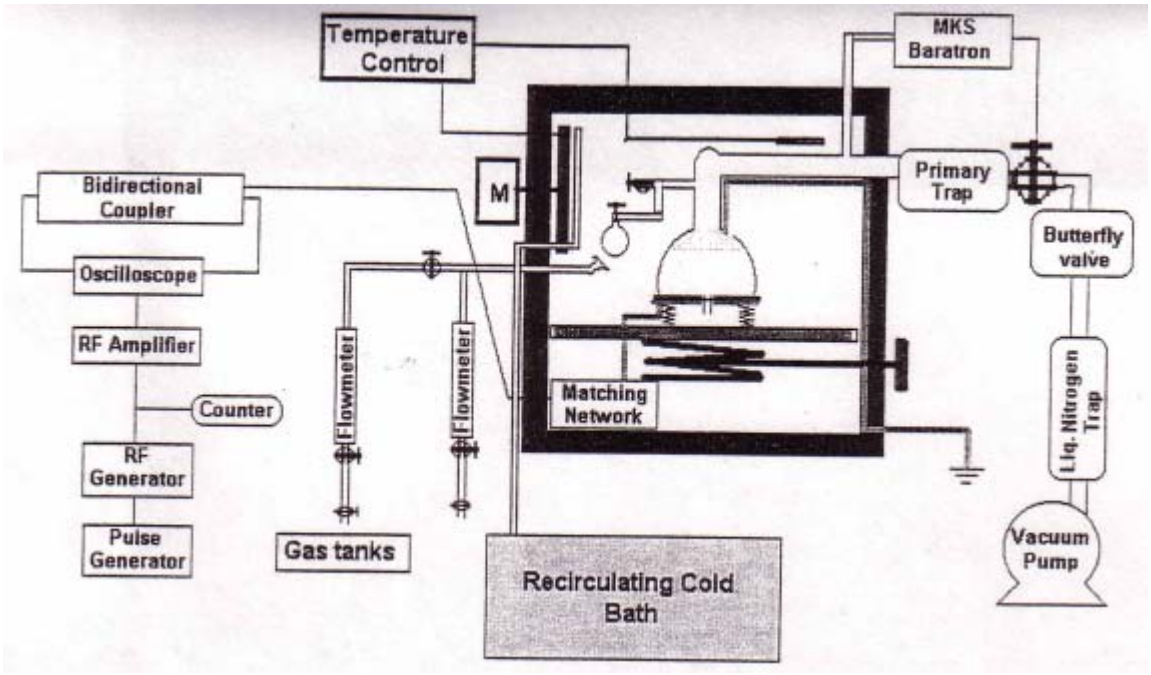

Fig. 2.3 Schematic diagram of heatable plasma reactor system

Prior to plasma polymerization, the system was evacuated to a background pressure of approximately 5 mtorr. This was followed by a 15 minutes pulsed argon plasma discharge at an Ar pressure of 400 mtorr, plasma peak power of 150 W and duty cycle 10/100 ms used to clean and activate the substrate surface (PEEK, PET or powder). After this cleaning step, the system was re-evacuated to the background pressure. Reactant monomer was then introduced into the reaction chamber and the glow discharge was ignited once the desired monomer pressure was set. After each experiment, the substrate was removed and reactor chamber was evacuated to background pressure and vented to the atmosphere. The reactor chamber was then cleaned, first with acetone, then

followed by an oxygen plasma at O_2 pressure of 400 mtorr, plasma peak power of 150 W and duty cycle 10/150 ms to remove any remaining polymer deposits in the interior of the plasma reactor.

Substrates materials employed included poly (ethylene terephthalate) (PET), poly (ether ether ketone) (PEEK), polished silicon wafers and KBr discs. The polymer substrates were mostly used in the solventless adhesive tests. Polished Si wafers were used for film thickness measurements, and KBr for FTIR measurements. XPS measurements were carried out on Si wafers. Prior to use, all substrates were subjected to ultrasonic cleaning in acetone solution. The KBr discs were also subjected to hand-polishing using acetone on soft tissue papers.

2.2 Plasma Deposition Conditions

2.2.1 Pulsed plasma polymerization of maleic anhydride

Anhydride groups were introduced onto a PEEK surface by pulsed plasma polymerization of maleic anhydride monomer:

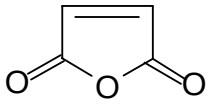

It was possible to identify operating conditions which provided deposition of well-defined anhydride functionalized films. The monomer input pressure, before plasma initiation, was approximately 76 mtorr. The pulsed plasma polymerization of maleic anhydride was performed at peak power of 50 W, and plasma on/off ratio of 0.2 ms and 12 ms.

It was anticipated that this film, functionalized with anhydride groups, would readily undergo reaction with amine-terminated nucleophiles coated on a second

substrate to produce surface amide linkages that convert into cyclic imide groups upon heating.

Maleic anhydride was purchased from Sigma-Aldrich Co.and used without any purification procedure other than standard degassing.

2.2.2 Pulsed plasma polymerization of glycidyl methacrylate

Polymeric films containing epoxide groups were prepared by plasma polymerization of glycidyl methacrylate (hereafter referred to as GM):

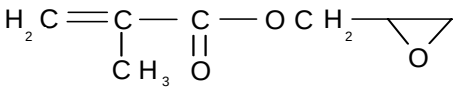

Pulsed plasma polymerization of GM was employed to deposit epoxide groups onto PEEK substrates. Experiments were conducted to identify reaction conditions that provide polymeric film having high epoxide group density. The retention of the epoxide groups were desired so that they might serve as an effective adhesion promoter through chemical bonding, e.g. to amine groups. The input monomer pressure of GM, prior to plasma initiation, was typically about 130 mtorr. The pulsed plasma polymerization experiments were carried out at peak power of 100 W, plasma on/off ratios of 10/50 ms, and 0.2/200 ms.

In order to get a stronger adhesive bonding between two PEEK substrates, the pulsed plasma polymerization of the mixture of glycidyl methacrylate and methacrylic acid ($H_2C=C(CH_3)COOH$)(3:1) was attempted. The input pressure of the monomer mixture was ~ 200 mtorr before plasma initiation. The pulsed plasma polymerization of the mixture monomer was performed at peak power of 100W, plasma on/off ratio of 10 ms and 50 ms. Glycidyl methacrylate and methacrylic acid were purchased from Sigma-

Aldrich Co. and used without any purification procedure other than standard degassing.

2.2.3 Pulsed plasma polymerization of ethylenediamine

Polymeric films containing amine groups were prepared by the pulsed plasma polymerization of ethylenediamine: $H_2NCH_2CH_2NH_2$. This monomer was employed to deposit amine groups onto PEEK substrates. The input pressure of ethylenediamine prior to plasma initiation was 210 mtorr. The pulsed plasma polymerization process was undertaken at peak power of 100W, and plasma on/off ratio of 10 ms and 150 ms. Ethylenediamine was purchased from Sigma-Aldrich Co. and used without any purification procedure.

2.2.4 Pulsed plasma polymerization of citraconic acid

The most extensive studies of plasma polymerization of citraconic acid ($CH_3C(COOH)=CHCOOH$) were carried out at input monomer pressure of 300 mtorr prior to plasma initiation, peak power of 100 W. To investigate the effect of plasma pulsing on the controllability and variation of polymer chemistry, the experiments were performed over a wide range of plasma duty cycles (1/5 ms to 1/100 ms). All experiments were performed in the high temperature plasma system. The temperatures of system and monomer during coating were at 80-Celsius degree. Citraconic acid was purchased from Sigma-Aldrich Co.

2.2.5 Pulsed plasma polymerization of 1,1,1-trichloroethane

The plasma polymerization of 1,1,1-trichloroethane was initially carried out at a monomer pressure of 110mtorr, and a peak power input of 100W. Polymerizations were undertaken over a wide range of RF duty cycles, in which a constant RF on time of 10ms was employed and the off time was varied systematically from 25 to 500ms.

Subsequently, to study the effect of plasma peak power on the controllability of polymer film chemistry, polymerizations were performed at a monomer pressure of 110 mtorr, and a fixed duty cycle of 10/25 ms, but varied peak power from 10 W to 200 W. Also, the effect of substrate temperature on the plasma polymerization was evaluated. To do so, polymerizations were carried out at a constant monomer pressure of 110 mtorr, a fixed peak power input of 100 W, and a fixed duty cycle of 10/25 ms, but with a changing coating temperature ranging from room temperature to 118 Celsius degree.

All of experiments were performed in the high temperature plasma system. 1,1,1-trichloroethane was purchased from Sigma-Aldrich Co.

2.2.6 Pulsed plasma polymerization of allylamine

Polyallylamine films for solventless adhesive use were undertaken at a monomer pressure of 220 mtorr. The peak power input was at 200 W, and the plasma on/off ratios were at 10/40 ms for 30 min and then at 10/200 ms for another 10 min.

Plasma polymerization of allylamine was also used to functionalize the surfaces of γ–Fe_2O_3 nanoparticles. Allylamine was polymerized under a constant monomer pressure of 300 mtorr via the baratron-controlled butterfly valve located downstream of the plasma reactor. The peak power input was at 100 W, and the plasma on/off ratios were at 10/40 ms and 10/100 ms.

Allylamine (98%) was purchased from Sigma-Aldrich Co. and used without any purification procedure. Gamma iron (III) oxide, was purchased from Marketech International Inc., and consisted of an average particle size of 35nm.

2.3 Characterization of Plasma Polymer Films

2.3.1 XPS and FT-IR spectroscopy

The film chemical compositions were characterized mainly using X-ray Photoelectron Spectroscopy (XPS) and Fourier Transform Infrared (FTIR) Spectroscopy.

The XPS spectra were obtained on a Perkin-Elmer PHI 5000 series spectrometer equipped with an X-ray source monochromator. The X-ray source employed is an Al Kα at 1486.6 eV. A pass energy of 17.90 eV, giving a resolution of 0.6 eV with Ag ($3d_{5/2}$), was used. Spectra were usually obtained at a pass energy of 8.95 eV using a 45º take-off angle. An electron flood gun (neutralizer) was employed to neutralize charge build-up on the insulator type films produced in the plasma deposition. The electron gun was operated under conditions to provide optimum resolution of the C (1s) peaks. Typical operating conditions for the neutralizer were 22.0 mA emission current and 1.8 eV electron energy. The XPS spectra of the plasma polymer films were standardized by centering the lowest binding energy peak in the C (1s) multiplets to 284.6 eV, which represents the binding energy of C atoms bonded exclusively to other C or H atoms.

Quantitative analysis of elemental compositions of deposited films was achieved by XPS analysis in a low-resolution survey scans. The atomic concentrations of surface elements were obtained by measuring the peak areas of the inner-level electrons, coupled with known instrument sensitivity factors for each element. Quantitative analysis of the functional group content of deposited films was achieved using the high-resolution scan mode. High-resolution XPS spectra of C (1s) permit a detailed characterization of the distribution of carbon atoms in plasma polymer films for different bonding structures. The binding energy shifts are related to the molecular environments of the carbon atoms.

A Bruker Vector 22 FT-IR spectrophotometer was employed for infrared analysis. FT-IR spectra were recorded at $4cm^{-1}$ resolution and 16 scans of films deposited on KBr discs from plasma polymerization process.

2.3.2 Film thickness and deposition rate

The film thicknesses of polymers deposited on silicon wafers were measured using a Tencor Alpha Step 200 profilometer. First, forceps were used to scribe a narrow scratch on the plasma-generated films. Then, the profilometer stylus scanned the scratched surface at a scanning rate of 50 μm/min over a 400μm scan range. Final film thickness was the average thickness that was achieved from the measurements at different locations on the film surface. Film deposition rates were calculated from the film thickness divided by coating time. (Å/min)

Film thickness growth per unit RF energy input (mÅ/J) was also calculated. It is calculated from:

$$Thickness(\overset{o}{A}) \Big/ \left(\frac{t_{on}}{t_{on} + t_{off}} \right) \times T_{coating}(\min) \times 60(s/\min) \times P_{peak}(J/s)$$

Where t_{on} and t_{off} are the plasma on and off times, $T_{coating}$ is the total elapsed time during plasma deposition and P_{peak} is the power input during t_{on}.

2.3.3 Contact angle measurement

The wettability of the plasma films was evaluated using static water contact angle measurements at room temperature. The static experiments involved use of a Ramé-Hart goniometer and measurements of advancing water contact angles. Advancing angle was recorded after each 4μl water drop addition to the surface to a total volume of 16μl.

2.3.4 Time-of-flight secondary ion mass spectroscopy (TOF-SIMS)

The analysis of surface elemental and chemical composition of the amine group functionalized γ-Fe_2O_3 nanoparticles was achieved by time-of-flight secondary ion mass spectroscopy. Measurements were obtained on TOF-SIMS IV manufactured by CAMECA/IONTOF, Germany.

2.3.5 Transmission electron microscope (TEM)

A JEOL-2011 Transmission electron microscope, with resolution better than 0.18 nm, was used to examine the polyallyamine film structures and their film thickness deposited on the surface of γ-Fe_2O_3 nanoparticles by pulsed plasma polymerization.

2.3.6 Particle size distribution analyzer (PSD)

The particle size distributions of γ-Fe_2O_3 nanoparticles, before and after coating, were obtained using the Mastersizer 2000 made by Malvern Instruments Ltd, which can measure particle dispersions and emulsions ranging in size from 20 nm to 2000 μm.

2.3.7 BET surface area measurement (Brunauer-Emmett-Teller)

The BET surface areas of γ-Fe_2O_3 nanoparticles before and after coatings by the pulsed plasma polymerization of allylamine were determined by nitrogen adsorption using an ASAP 2400 Micromerit instrument.

Note: The TOF-SIMS, TEM, PSD and BET measurements were carried out at the Dupont Corp. Central Research and Development labs, located in Wilmington, DE.

CHAPTER 3

RESULTS AND DISCUSSION

3.1 Molecular Tailored Ultra Thin Films for Use in Covalent Adhesive Bonding

The objective of this work was to develop an all-dry ultra-thin film process to bond polymeric substrates (PEEK). It involved systematic studies of experimental variables to optimize adhesive properties of these films, consistent with maintaining minimal film thickness. The pulsed plasma approach was employed to synthesize thin films containing reactive functional groups. The basic idea was to deposit different functional groups on each substrate and subsequently bond the substrates via simple covalent bond formation between the two plasma deposited films. For example, if film A contained epoxide groups and film B contains amine group, it should be possible to react these two films via formation of secondary alcohol bonds between these two reactive groups. The pulsed technique is employed as it has been shown, using unsaturated functionalized monomers, that it is possible to conserve relatively high percentages of the reactive functional groups in the polymeric films when low duty cycle (low average power input) conditions are employed. The reactive groups investigated included anhydride, epoxide, carboxyl and amine groups.

3.1.1 Adhesion between anhydride and amine groups

First, anhydride groups were introduced onto a PEEK surface by pulsed plasma polymerization of maleic anhydride monomer. It was possible to identify operating

conditions, which led to the deposition of well-defined anhydride functionalized films. The relatively high structural retention of anhydride groups in the film was confirmed by IR analysis. (See Fig.3.1)

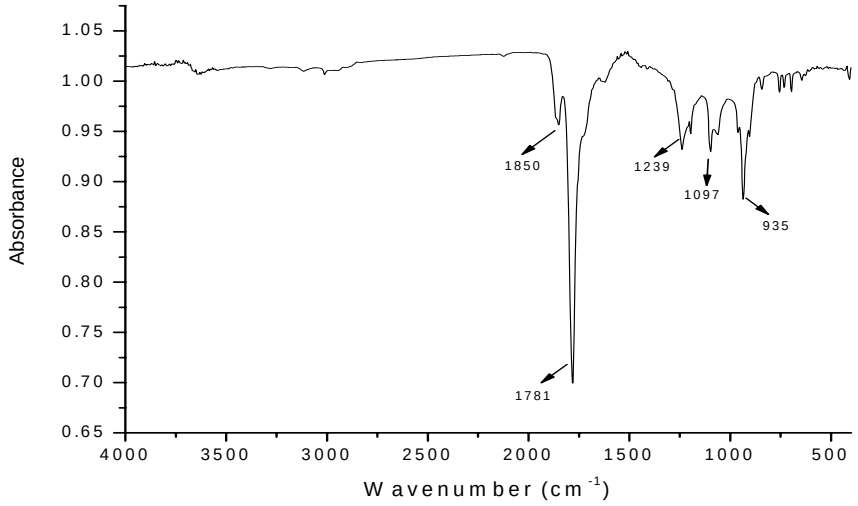

Fig. 3.1 FTIR spectrum of pulsed plasma maleic anhydride at a peak power of 50W with duty cycle of 0.2/12ms

Figure 3.1 is the FTIR spectrum of the plasma polymerized maleic anhydride film deposited on a KBr disc. IR absorption bands at 1781cm^{-1} and 1850cm^{-1} are the asymmetric and symmetric stretching vibrations of the anhydride group. [20] [46] C-O-C stretching vibration appears at 1239cm^{-1} and the absorption band at 935cm^{-1} belongs to cyclic unconjugated anhydride. As shown in this spectrum, the anhydride groups required for the subsequent adhesion reaction were retained very well by the pulsed plasma polymerization of maleic anhydride.

It was anticipated that this film would readily undergo reaction with amine-terminated nucleophiles coated on a second substrate to produce surface amide linkages that convert into cyclic imide groups upon heating. (The proposed reaction is shown in

Fig. 3.2.)

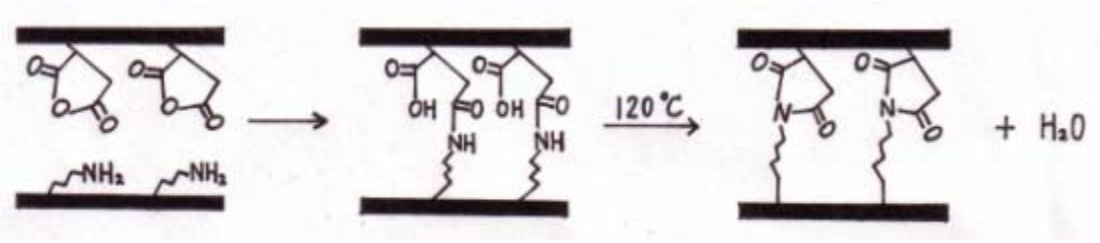

Fig. 3.2 Schematic diagram of the reactions carried out between anhydride groups coated PEEK substrates and amine groups coated PEEK substrates

Amine functionalized PEEK substrates were obtained by pulsed plasma deposition of ethylenediamine monomer. The preservation of the amine functional groups during the polymer formation was indicated by IR spectroscopy. (See Fig. 3.3)

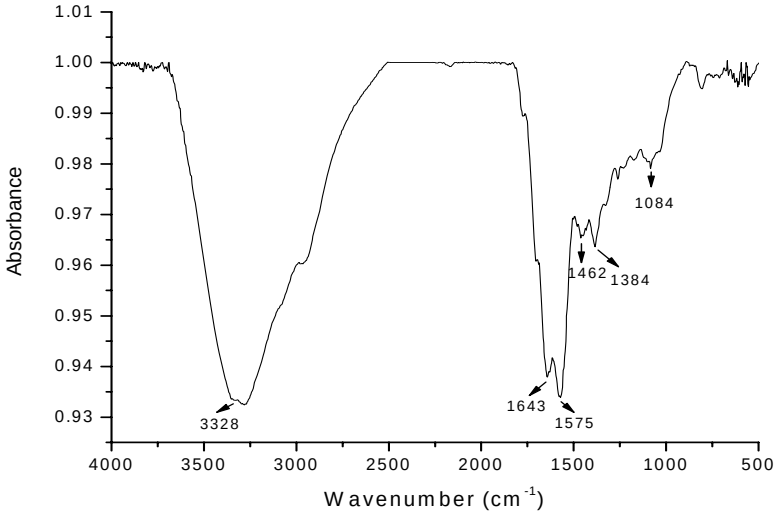

Fig. 3.3 FTIR spectrum of pulsed plasma ethylenediamine deposited at a peak power of 100 W with duty cycle of 10/150 ms

Fig.3.3 is the FTIR spectrum of the plasma polymerized ethylenediamine film deposited on a KBr disc. The strong broad absorption band around 3328cm^{-1} is the characteristic N-H stretching vibration. The band at 1643cm^{-1} belongs to the amine N-H deformation vibration. In addition, the amine C-N stretching vibration band is at 1084

cm^{-1}. The FTIR spectrum of plasma polymerized ethylenediamine shows that the amine groups were retained during the plasma polymerization process.

The bondability of modified PEEK surfaces was evaluated by joining the two PEEK substrates, separately coated by maleic anhydride and ethylenediamine. These substrates were then cured overnight at 120°C under a constant load of about 0.6 Kg/cm^2. Subsequently, they were allowed to cool to room temperature over a 5 hour period. Adhesive bonding between the two modified PEEK substrates was obtained, but the bond strength was obviously weak as relatively little force was required to separate overlapped substrates.

3.1.2 Adhesion between epoxide and amine groups

Epoxide functional groups were then evaluated to serve as an effective adhesion promoter through chemical bonding. In light of commercially available epoxy based cement, surface epoxide groups should provide strong bonding sites for nucleophile reagents, such as amines. (The proposed reaction is shown below)

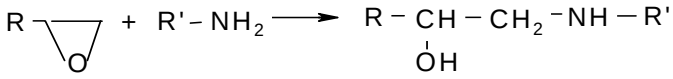

Pulsed plasma polymerization of glycidyl methacrylate was employed to deposit epoxide groups onto PEEK substrates. Experimentation was undertaken to identify plasma reaction conditions which optimized epoxide functional group retention in the polymer films. Surprisingly, IR spectral results obtained indicated that relatively high epoxide surface densities were obtained at both low (0.2/200ms) and high (10/50ms) plasma on/off ratios, and 100W peak power. (See Fig. 3.4) Relatively similar FTIR spectra were obtained from glycidyl methacrylate polymerized films at these two

different plasma duty cycles. The broad band around 3500cm^{-1} is attributed to the O-H stretching vibration band; the strong absorption band at 1730cm^{-1} is the characteristic stretching vibration of C=O group; the C-O-C stretching vibration band in glycidyl methacrylate molecule is at 1149cm^{-1}. The absorption bands at 1257cm^{-1} (C-O stretching) and 851cm^{-1}, 908cm^{-1} (ring vibration) show the presence of epoxide groups on the polymer film deposited from the pulsed plasma polymerization of glycidyl methacrylate. (20a)

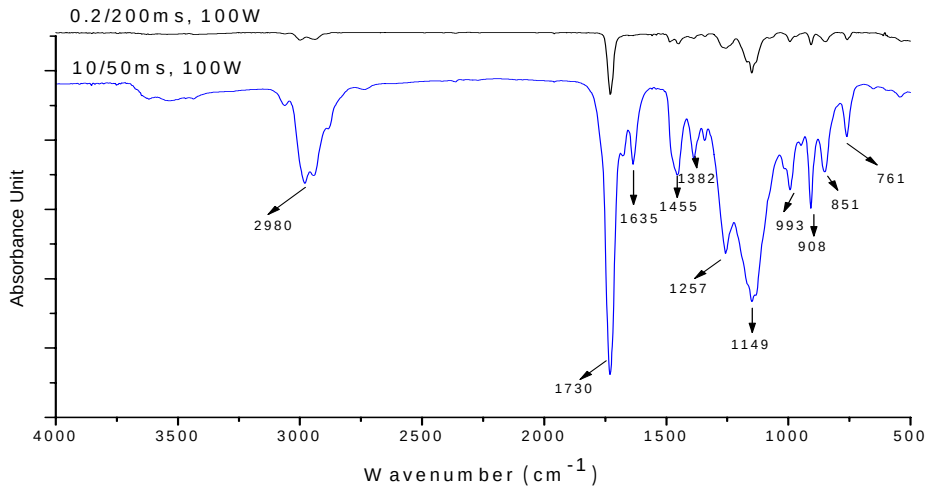

Fig. 3.4 FTIR spectra of pulsed plasma glycidyl methacrylate deposited at a peak power of 100W with duty cycles of 0.2/200 ms and 10/50 ms

Amine functionalized PEEK substrates were obtained by pulsed plasma deposition of allylamine monomer. The preservation of a significant amount of the amine functional groups in the plasma-generated polymer was indicated by IR spectroscopy. (See Fig. 3.5) The broad absorption band around 3339cm^{-1} is N-H stretching vibration; the band at 1632cm^{-1} belongs to the amine N-H deformation vibration; primary amine C-N stretching vibration band is at 1033cm^{-1}. In addition, absorption bands at 2931cm^{-1}(C-

H stretching vibration), and 1452cm^{-1}, 1376cm^{-1}(C-H bending) are characteristic absorption bands of hydrocarbons. The absorption bands at 1115 cm^{-1} and 1156 cm^{-1} would be consistent with the presence of secondary amine functional group.

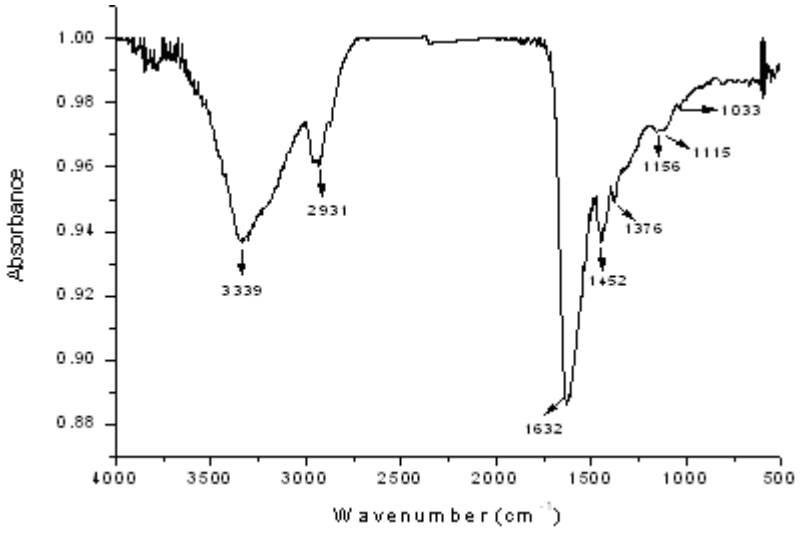

Fig. 3.5 FTIR spectrum of pulsed plasma allylamine deposited at a peak power of 200W with duty cycles of 10/40ms (30min) and 10/200ms (10min)

The bondability of modified PEEK surfaces was evaluated by joining the two PEEK substrates, separately coated by glycidyl methacrylate and allylamine. These substrates were then cured overnight at 120˚C under a constant load of about 0.6 Kg/cm^2. Subsequently, they were allowed to cool to room temperature over a 5 hour period. Adhesive bonding between the two modified PEEK substrates was obtained. Peel force of the adhesive bond was 1.5 lb/inch. The increased adhesive bonding, compared with that between maleic anhydride and ethylenediamine, was attributed to the presence of secondary alcoholic bonds from the reactions of epoxides and amine groups and the presence of hydrogen bonds between the products, which would further enhance the adhesive bonding between the two-coated substrates.

The strongest adhesive bonding obtained between two PEEK substrates was from the pulsed plasma polymerization of the mixture of glycidyl methacrylate (GM) and methacrylic acid (MA) (3:1) instead of the pure glycidyl methacrylate monomer. The operating variable of pulsed plasma technique was the same as that for pure glycidyl methacrylate (10/50ms, 100W).

The reaction between surface epoxide groups and amines was further investigated using ethylenediamine as a coupling agent in lieu of allylamine for adhesion. A drop of 0.5 M solution of ethylenediamine dissolved in 1,4-dioxane was placed between two pieces of plasma (GM+MA) coated PEEK substrates. The samples were then heated overnight at 120°C under a constant load of about 0.6Kg/cm^2 to allow solvent evaporation and bonding. They were cooled to room temperature over 5 hrs. Adhesive bonding between the two plasma coated PEEK substrates was obtained. Peel force measurement indicated that the peel force is 1.8 lb/inch.

This is a highly encouraging result. It strongly suggests that the carboxyl groups in methacrylic acid play an important role in the enhanced adhesion. It is assumed that the carboxyl groups react with the amine groups in the coupling reagent to form salt or amide (under heating) and they also react with epoxide groups in glycidyl methacrylate at the same time with the formation of secondary alcohol between epoxides and amines. Additionally, hydrogen bonds would also be expected to contribute to the enhanced adhesion. (The proposed reactions are shown in the following page.)

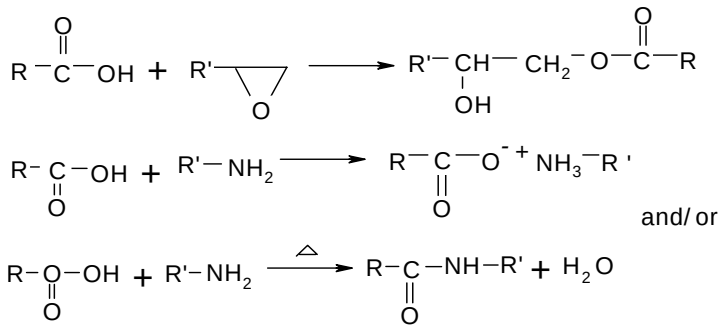

3.2 Surface Carboxylation by Pulsed Plasma Polymerization of Citraconic Acid

The objective of this study was to employ the pulsed plasma polymerization of a monomer containing two carboxyl groups to produce a coating having a high and controllable surface density of carboxylic functional groups. This study represents the first attempt to plasma polymerize a di-carboxylic acid.

Variations in film compositions with variations in duty cycles were observed for polymers obtained during plasma polymerization of the citraconic acid monomer. These variations were revealed by XPS and FTIR spectral analysis of these polymers, both of which confirmed the presence of COOH groups in these films.

The elemental survey scans of the plasma-polymerized citraconic acid surfaces showed that the films were composed of carbon and oxygen atoms. Figure 3.6 shows a deconvoluted high resolution C(1s) XPS spectrum of plasma polymerized citraconic acid deposited at a duty cycle of 1/40ms and a peak power of 100W. The table 3.1 shows the binding energy and full widths at half-maximum (FWHM) of the various functional groups. In the polymerized citraconic acid film, carbon environments of the form C-R, C-O, C=O, and COOR (R=H or C) were expected to be present, each exhibiting a characteristic chemical shift (or chemical bonding energy). Because of the high

electronegtivity of the carboxyl group, one can also expect an environment of the type C-COOR to be distinguishable from a purely hydrocarbon one. [45]

Table 3.1 The Binding Energy and Full Widths at Half-Maximum (FWHM) of The Various Functional Groups Obtained from High Resolution C(1s) Spectra of Pulsed Plasma Polymerized Citraconic Acid Films

Carbon Environment	Peak Position (eV)	FWHM	Proportion Of C(1s) Area
C-R (R=H or C)	284.90	1.498	61.901
C-COOR	285.29	1.505	7.991
C-O	286.27	1.603	14.679
C=O	287.67	1.607	7.734
COOR	289.26	1.508	7.902

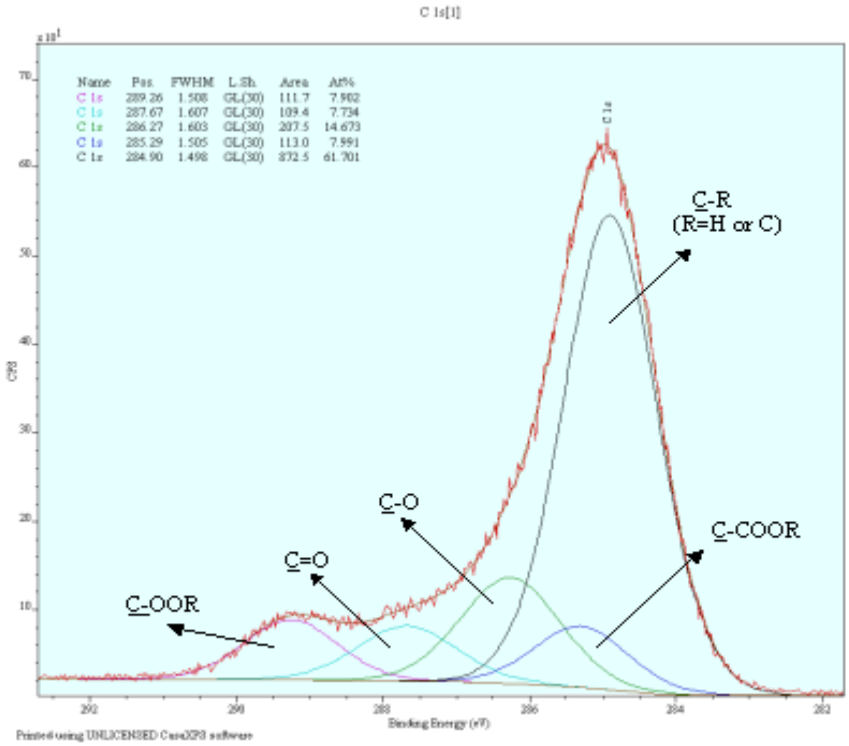

Fig. 3.6 High resolution C(1s) XPS spectrum of pulsed plasma polymerized citraconic acid film at a duty cycle of 1/40ms and a peak power of 100W

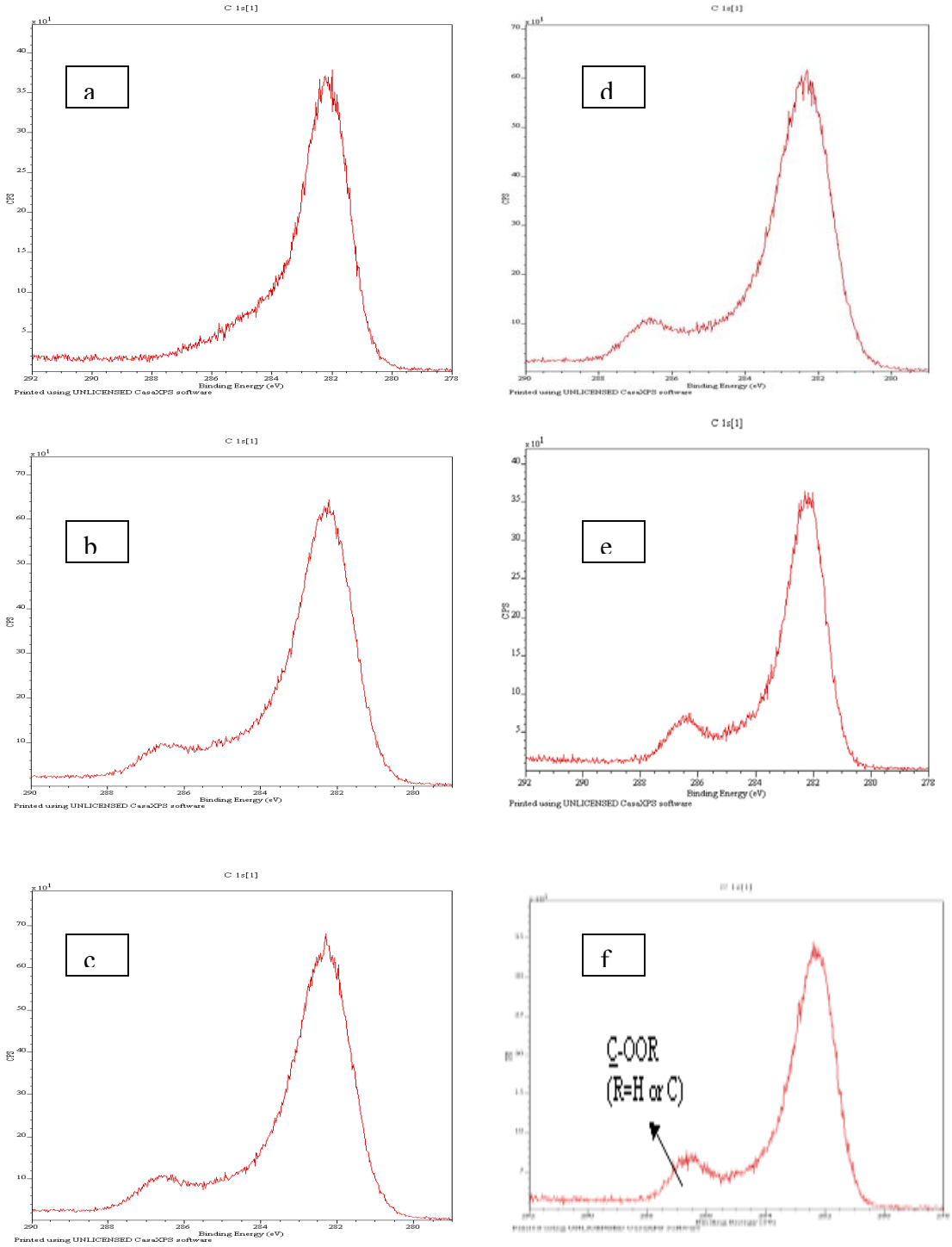

Fig. 3.7 High resolution C(1s) XPS spectra of pulsed plasma citraconic acid films at various duty cycles ranging from 1/5ms to 1/100ms,as indicated. All films were polymerized at a peak power of 100W; (a) 1/5ms (b) 1/20ms (c) 1/30ms, (d) 1/40ms (e) 1/50ms (f) 1/100ms

The high resolution C(1s) XPS spectra of citraconic acid films polymerized at a constant peak power of 100W, arranged in the order of increasing plasma off time, are shown in figure 3.7. Table 3.2 illustrates the relative concentrations of all carbon environments of these films obtained at different duty cycles. As shown in Figure 3.7 and Table 3.2, the relative content of carboxylic groups in these films obtained from peak areas of the C-OOR (R=H or C) groups at 289.26eV, can be progressively increased in a controllable manner over the range of duty cycles employed. Figure 3.7 shows that a relatively higher retention of carboxylic groups (COOR) was achieved at a lower plasma duty cycle, all other plasma variables being held constant.

Table 3.2 High Resolution C(1s) XPS Results of Pulsed Plasma Polymerized Citraconic Acid Films Obtained at Different Duty Cycles

Duty Cycles (ms)	Relative Concentrations (%)				
	COOR	C = O	C – O	C	C-R
	289.26	287.63	286.21	285.32	284.90
1/5	4.04	8.20	18.60	4.02	65.15
1/20	7.90	7.73	14.67	7.99	61.70
1/30	9.17	7.66	13.43	9.16	60.59
1/40	9.77	7.60	12.87	9.58	60.19
1/50	11.13	7.37	12.30	11.28	57.93
1/100	11.65	7.12	11.43	12.24	57.56

The high bonding energy peak at 289.26eV is attributed to carboxyl functionality (COO^-) and would include contributions from both carboxylic acid (COOH) and ester (COOC) groups. Studies in plasma polymerization of acrylic acid have shown that the

ester group may be present in plasma-polymerized films. [45] In the present case, the C-O film content is much higher than that of COOH (or COOR) at high duty cycles indicating fragmentation of the monomer is significant. However, the relative concentration of carboxyl groups to C-O groups increases, as the duty cycle is decreased, consistent with increasing retention of the carboxyl group in the polymer films with decreased duty cycle.

FTIR spectral characterization also provided evidence of plasma polymerized citraconic acid film chemistry variation with duty cycle variations during polymerization. Figure 3.8 shows FTIR spectra of pulsed plasma citraconic acid films deposited on KBr discs, arranged in the order of increasing off time during deposition from top to bottom.

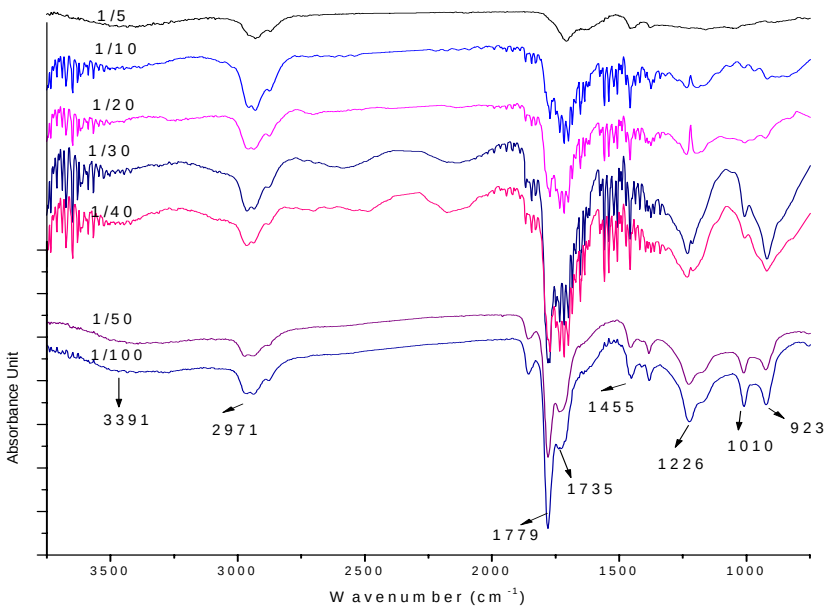

Fig. 3.8 FTIR spectra of pulsed plasma citraconic acid films at a peak power of 100W with duty cycles ranging from 1/5 to 1/100 ms

The relatively broad absorption band around 3391cm^{-1} is characteristic of the presence of -COOH groups. It indicates that carboxylic acid groups are present in all films generated from plasma polymerization of citraconic acid at different duty cycles. The split sharp bands at 1779 cm^{-1}and 1735 cm^{-1} from carbonyl stretch are typical absorption bands of a dicarboxylic acid. [46] The relative intensity of the band at 1779cm^{-1} decreased progressively as the duty cycle, or average power input is increased. At a duty cycle of 1/5 ms, it is not present as only one carbonyl stretch band (1735 cm^{-1}) remains. The FT-IR results indicate that dicarboxyl functionalities were gradually destroyed when the average input power conditions during deposition became more energetic. One of carboxyl groups in this molecule was lost as carbon dioxide or carbon monoxide during the energetic plasma discharge. In addition, the relative intensities of the C-H stretching vibrations, at 2971 cm^{-1}, became more pronounced as the duty cycle or average power input was increased. The IR results are confirmed by the ESCA data, which reveal the relative concentration of -COOH is the least at 1/5 ms. (Table 3.2)

The concentration variations of carboxylic content in citraconic acid plasma polymerized films, as functions of off time and average power input, are shown in Figure 3.9. The concentration of carboxylic content is gradually increased with increased off time, and decreased as the average power input during deposition is increased. This result is consistent with formation of more highly cross-linked polymeric film as the power input is increased. It shows that the average power input during plasma polymerization plays an important role in controlling the chemical composition of plasma films. But the relatively low overall retention of carboxylic group, coupled with the low volatility of the

monomer make citraconic acid not a good candidate for the purpose of creating surfaces having high surface densities of –COOH groups.

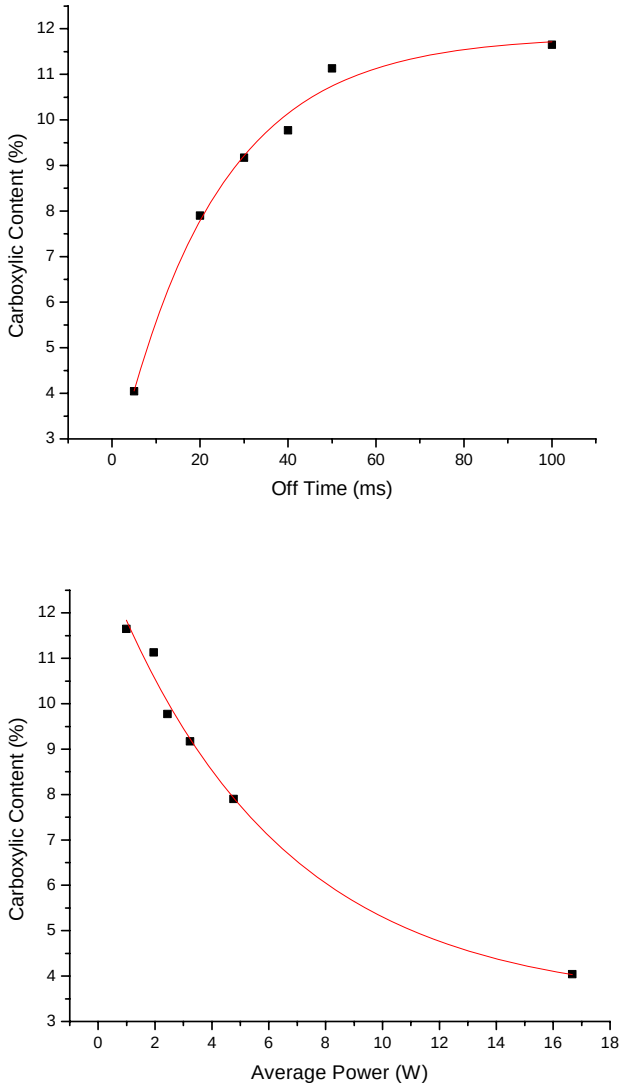

Fig. 3.9 Concentration variations of carboxylic contents in citraconic acid plasma polymerized films as a function of off time and as a function of average power input, expressed as a percentage of the total surface carbon atom content

3.3 Amine Groups (-NH_2) Functionalized γ-Fe_2O_3 Nanoparticles by Pulsed Plasma Polymerization Process

The long range of objective of this work is to use surface modified super paramagnetic nanoparticles, gamma iron oxide, as site-specific drug carriers. Super paramagnetic particles do not retain magnetization before and after exposure to an external magnetic field, reducing the possibility of particle aggregation due to magnetic attraction, and providing a good approach to drug delivery to a specific site by use of an external magnetic field. To improve the biocompatibility and dispersion of nanoparticles in biological environments, and to immobilize foreign molecules on nanoparticle surfaces, nanoparticle surface modification is required. In the present study, amine groups were deposited on the nanoparticle surfaces by a pulsed plasma polymerization process. These amine groups would, in principle, be usable to immobilize foreign molecules or drugs and deliver them to specific organs.

3.3.1 Particle size distribution (PSD)

The effect of plasma polymerization on particle size distribution of the γ-Fe_2O_3 nanoparticles has been examined. Figure 3.10 shows PSD plots of uncoated γ-Fe_2O_3 nanoparticles and polyallylamine coated γ-Fe_2O_3 nanoparticles. The coating process was conducted at two duty cycles. As shown in Figure 3.10, most of uncoated γ-Fe_2O_3 nanoparticles show a particle size distribution centered around 5μm, with a smaller group centered around 600nm. Clearly, these particles are highly aggregated. After plasma deposition of allylamine, half of coated sample A, which was plasma polymerized at a peak power of 200W and duty cycles of 10/100ms, reveal particle distributions centered around 600nm and 1.1μm. The coated sample B, plasma polymerized at a peak power of

200W and duty cycles of 10/40ms, gave particle size distributions similar to those from sample A. The 200 μm size particles, indicated with all these samples, is an instrumental artifact which was present even in the absence of particles.

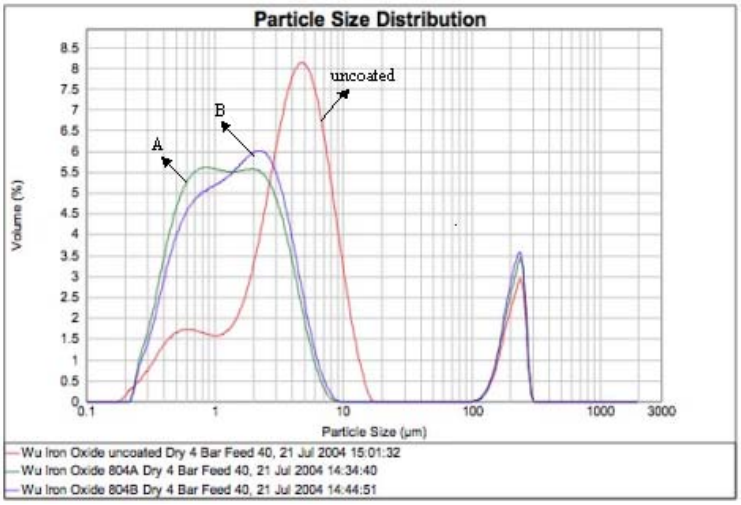

Fig. 3.10 Particle size distributions of uncoated γ-Fe_2O_3 nanoparticles and allylamine plasma polymerized γ-Fe_2O_3 nanoparticles at different duty cycles: A---10/100ms, 200W, B---- 10/40ms, 200W

The results indicate that the coated samples are somewhat smaller than the uncoated particles. These results provide evidence that the pulsed plasma polymerization process not only can functionalize nanoparticles but the coating process apparently helps to reduce particle aggregation.

3.3.2 Microscopic analysis of coated and uncoated γ-Fe_2O_3 particles

The morphology of γ-Fe_2O_3 nanoparticles and the structure of allylamine plasma polymerized films were studied by transmission electronic microscope. Figure 3.11 is the TEM image of the uncoated γ-Fe_2O_3 nanoparticles and Figure 3.12 is the TEM image of γ-Fe_2O_3 nanoparticles functionalized by allylamine pulsed plasma polymerization at a peak power of 200W and duty cycle of 10/100ms. As shown in these two images, the

surfaces of uncoated γ-Fe_2O_3 nanoparticles are bare whereas a thin amorphous structure covers the surfaces of allylamine plasma coated γ-Fe_2O_3 nanoparticles. This thin coating is attributed to the deposition of polymeric allylamine films during plasma treatment.

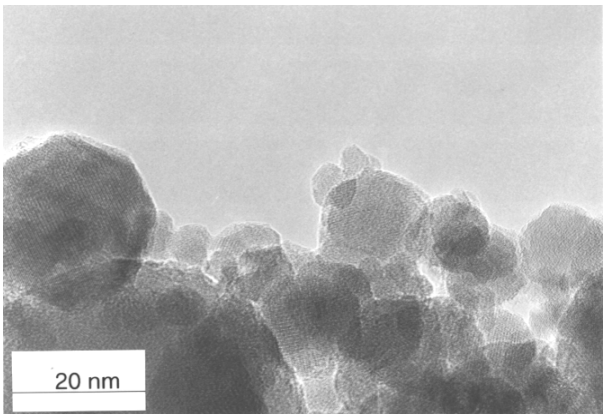

Fig. 3.11 TEM image of uncoated γ-Fe_2O_3 nanoparticles

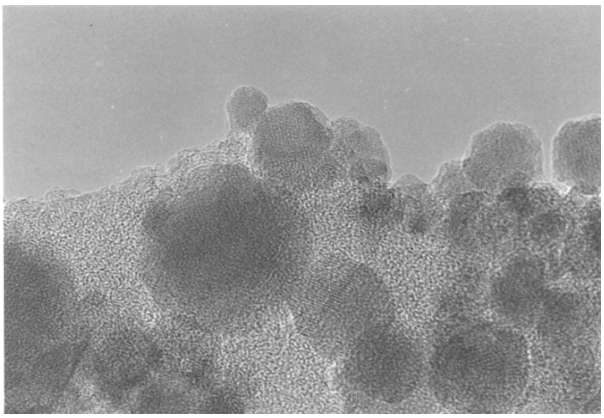

Fig. 3.12 TEM image of allylamine plasma polymerized γ-Fe_2O_3 nanoparticles at a peak power of 200W and duty cycle of 10/100ms

The effectiveness of the plasma deposition process in coating the γ-Fe_2O_3 nanoparticles was more clearly evident in pictures obtained by the high-resolution transmission electronic microscope (HRTEM). Figures 3.13 are HRTEM images of allylamine plasma polymerized γ-Fe_2O_3 nanoparticles at the same peak power of 200W

but different duty cycles: (a) 10/100ms, (b) 10/40ms. The polyallylamine amorphous structures in both of (a) and (b) are uniformly covering the surfaces of γ-Fe_2O_3 nanoparticle crystal. These polymer films are approximately 4 nm thick.

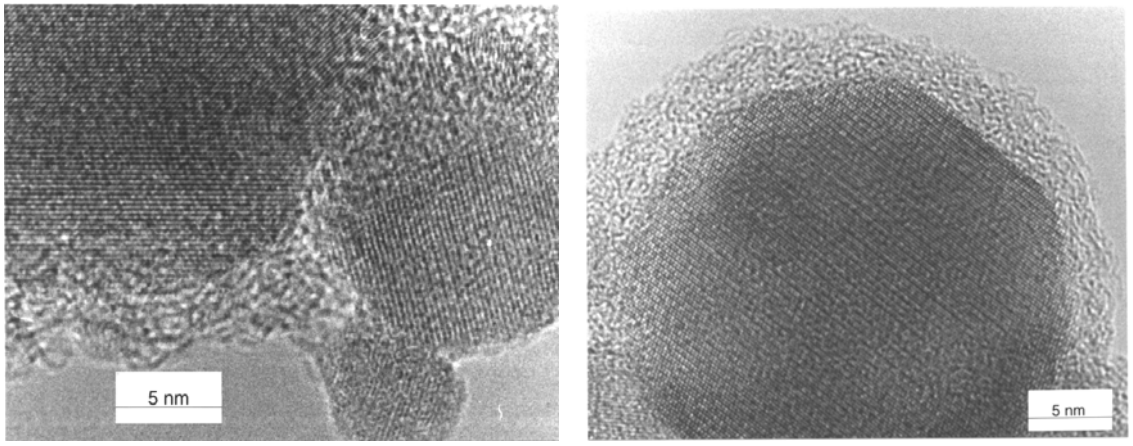

Fig. 3.13 HRTEM images of allylamine plasma polymerized γ-Fe_2O_3 nanoparticles at a peak power of 200W and duty cycle of (a) 10/100ms and (b) 10/40ms for 30min

3.3.3 Spectroscopic characterizations

Film compositional changes with variations in plasma duty cycles during deposition were observed for polymers obtained during plasma polymerization of the alllylamine monomer on γ-Fe_2O_3 nanoparticle surfaces. The film compositions were revealed by XPS, FTIR, ToF-SIMS spectral analysis, all of which confirmed the presence of amine groups in the films.

Figure 3.14 shows the FTIR of γ-Fe_2O_3 nanoparticles before and after coating with allylamine by pulsed plasma polymerization. The strong absorption bands at 688 cm^{-1}, 630cm^{-1} and 580cm^{-1}, observed in the infrared spectra of iron oxide nanoparticles with and without allylamine coating, confirmed that the dominant crystal phase of iron oxide in all three samples was γ-Fe_2O_3. [47] For γ-Fe_2O_3 nanoparticles without allylamine

coating, the broad band at 3410 cm^{-1} indicated the presence of surface hydroxyl groups. [39] The observed C-H stretching bands (2962 cm^{-1}, 2934 cm^{-1}) and C-H bending bands (1458 $cm^{-1}$and 1382 cm^{-1}) in the coated γ-Fe_2O_3 nanoparticles confirmed the presence of a hydrocarbon containing coating on the surface of the γ-Fe_2O_3 nanoparticles. But FTIR cannot prove the presence of amine groups since the band at 3345 cm^{-1} can be the N-H or O-H stretching vibration band, and the band at 1643 cm^{-1} can be N-H bending or C=C stretching vibration. So other spectroscopic techniques (XPS and ToF-SIMS) were utilized to analyze the film composition.

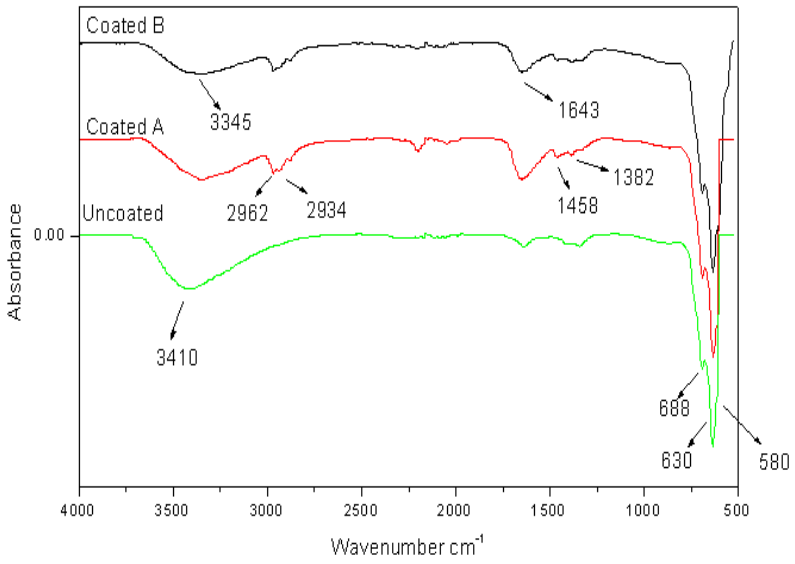

Fig. 3.14 FTIR spectra of uncoated γ-Fe_2O_3 nanoparticles and allylamine plasma coated γ-Fe_2O_3 nanoparticles at a peak power of 200W with different duty cycles: A---10/100ms; B---10/40ms

Figure 3.15 is the N1s high-resolution XPS spectra of γ-Fe_2O_3 nanoparticles before and after allylamine coating. There is no peak around 400eV, which is N1s characteristic binding energy, on the XPS spectrum of uncoated γ-Fe_2O_3 nanoparticles.

Obviously, there were no nitrogen atoms on the surfaces of uncoated γ-Fe_2O_3 nanoparticles. However, N1s high-resolution spectra of coated samples confirmed the presence of nitrogen atoms on iron oxide nanoparticles subjected to the allylamine plasma treatment. The atom percentage concentrations on surfaces of γ-Fe_2O_3 nanoparticles before and after coating were obtained from the XPS survey scans; the results are shown in table 3.3. As shown in table 3.3, the concentrations of carbon and nitrogen were increased significantly after allylamine plasma coating. In particular the concentration of nitrogen atoms on the surfaces of allylamine coated γ-Fe_2O_3 nanoparticles were 18 times more than that on the surfaces of uncoated sample.

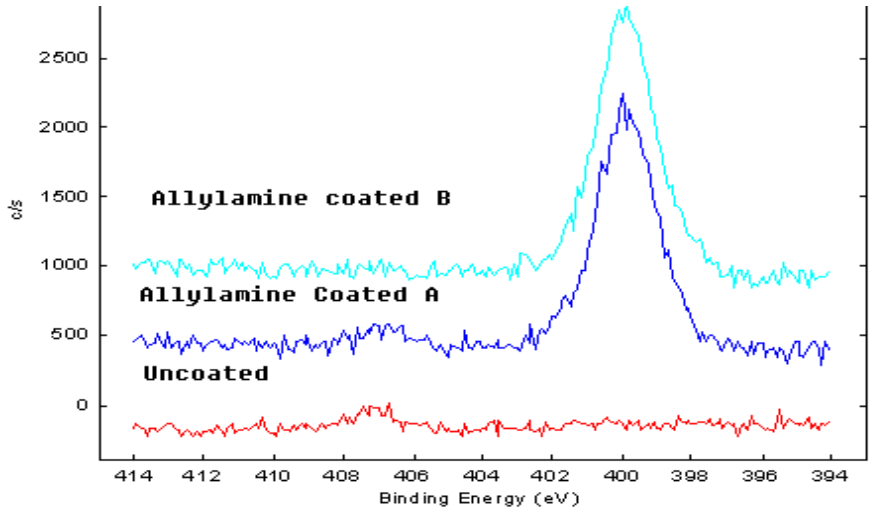

Fig. 3.15 N1s High resolution XPS spectra of uncoated γ-Fe_2O_3 nanoparticles and allylamine plasma coated γ-Fe_2O_3 nanoparticles at a peak power of 200W with different duty cycles: A---10/100ms, B---10/40ms

Table 3.3 XPS Results of Percentage Concentration of Atoms on the Uncoated γ-Fe_2O_3 Nanoparticle Surfaces and Those on the Allylamine Plasma Coated γ-Fe_2O_3 Nanoparticle Surfaces at a Peak Power of 200W with Different Duty Cycles: A---10/100ms, B---10/40ms

Samples	C	N	O	Fe	C/Fe	N/Fe
Uncoated γ-Fe_2O_3	39.0	0.3	36.0	21.8	1.8	0.01
Allylamine coated γ-Fe_2O_3, A	42.3	5.3	30.3	19.7	2.1	0.27
Allylamine coated γ-Fe_2O_3, B	47.2	5.4	28.8	16.5	2.9	0.33

XPS survey scans and N1s high-resolution spectra provided the evidence that allylamine had been plasma polymerized on the surfaces of γ-Fe_2O_3 nanoparticles. But the two samples polymerized at different duty cycles cannot be differentiated; they both gave similar film compositions. However, ToF-SIMS analysis of these samples confirmed that γ-Fe_2O_3 nanoparticles contain amine groups from the allylamine polymerization.

Figure 3.16 shows ToF-SIMS spectra of γ-Fe_2O_3 nanoparticles before and after allylamine plasma coating. Peaks at 27, 29, 39, 41, 43, 55, 57 represent hydrocarbon species. The $-NH_2$ containing species, such as those identified at masses of 18, 30, 42, and 44 are much stronger on the allylamine plasma coated γ-Fe_2O_3 nanoparticles samples. The peak at 73 belongs to FeOH, which confirms that there were-OH groups on the surfaces of uncoated γ-Fe_2O_3 nanoparticles. But this peak is very weak on the ToF-SIMS spectra of allylamine coated samples, this observation suggests that the absorption band at 3345cm^{-1} in the FTIR of allylamine plasma polymerized γ-Fe_2O_3 nanoparticles, is not a stretching band of O-H, but rather the stretching band of N-H. Overall, the ToF-SIMS

spectra confirm the presence of amine groups on the surfaces of the γ-Fe_2O_3 nanoparticles. In addition, the ToF-SIMS spectra of the plasma treated samples exhibit polymer characteristic spectra above 100 (m/z) and thus the presence of polymer film on the treated samples. ToF-SIMS spectra also can show the relative intensity of $–NH_2$ containing species versus Fe containing species, as shown in table 3.4.

Table 3.4 The Relative Intensity of $–NH_2$ Containing Species Versus Fe Containing Species from ToF-SIMS Spectra of γ-Fe_2O_3 Nanoparticles Before and After Allylamine Plasma Coating

Samples	R-NH_2/Fe (Relative Intensity)
Uncoated γ-Fe_2O_3	0.094
Allylamine Coated γ-Fe_2O_3, A (10/100ms, 200W, 30min)	0.896
Allylamine Coated γ-Fe_2O_3, B (10/40ms, 200W, 30min)	0.875

As shown in table 3.4, the relative intensity of amine groups containing species have been increased around 9 times more than that in uncoated samples after allylamine plasma coating on the surfaces of γ-Fe_2O_3 nanoparticles.

Combined, the FTIR, XPS and ToF-SIMS provided strong evidence that the surfaces of γ-Fe_2O_3 nanoparticles were functionalized during the allylamine pulsed plasma polymerization process and that the polymer coatings deposited contained amine groups.

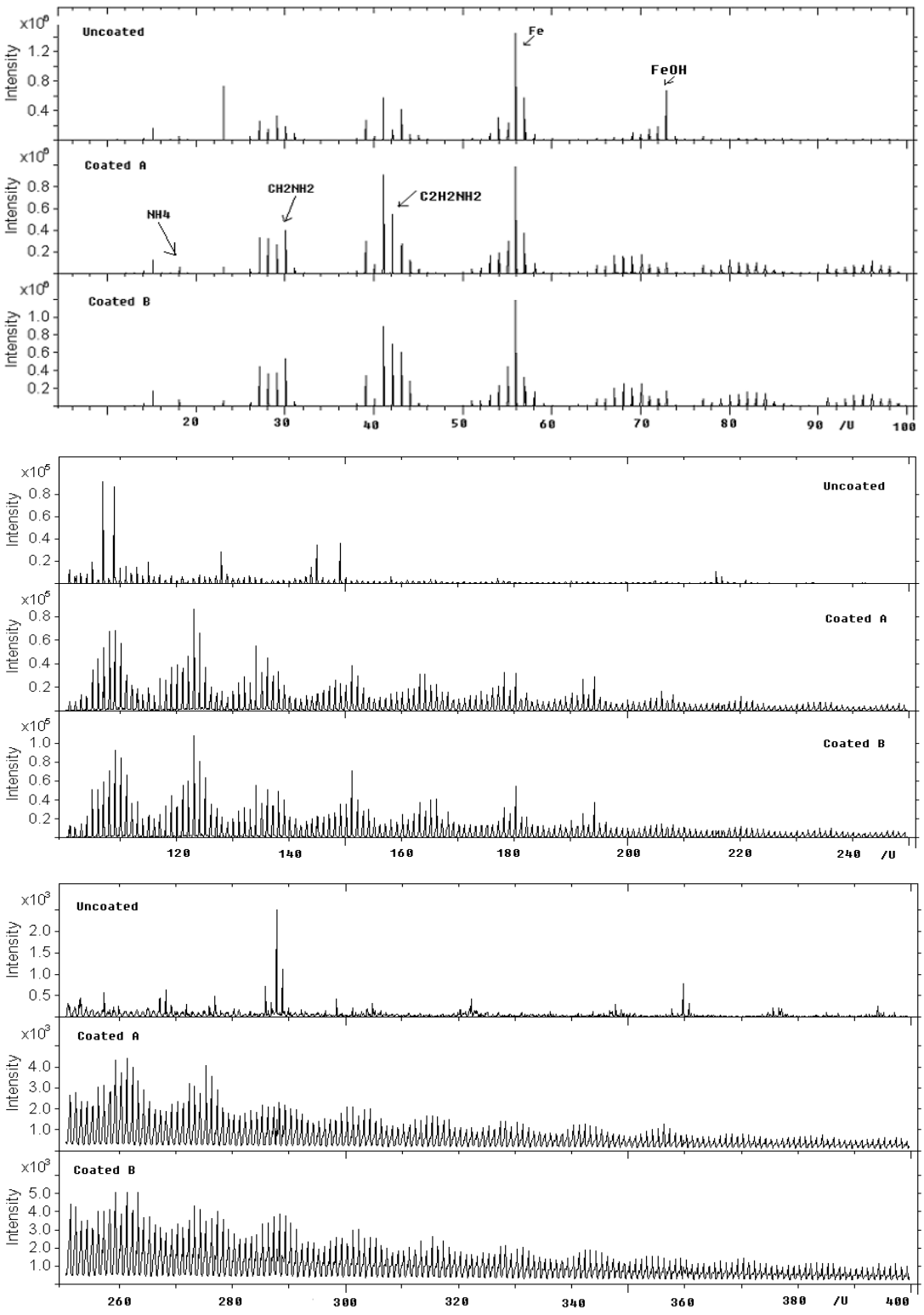

Fig. 3.16 ToF-SIMS spectra of uncoated γ-Fe_2O_3 and allylamine plasma coated γ- Fe_2O_3 nanoparticles at a peak power of 200W with different duty cycles: A---10/100 ms, B---10/40ms

3.3.4 BET surface area measurement

The BET surface areas of uncoated γ-Fe_2O_3 nanoparticles and polyallylamine coated γ-Fe_2O_3 nanoparticles at different duty cycles were also measured. The results are shown in Table 3.5. The uncoated γ-Fe_2O_3 nanoparticles have a 51.8 m^2/g BET surface area; after allylamine plasma coating, their BET surface areas were reduced to 44.2 m^2/g and 43.9 m^2/g. This result indicates that the plasma deposited polymer film on the surfaces of γ-Fe_2O_3 nanoparticles decreased the overall surface area of the particles, most likely by filling crevices and providing an overall smoother surface.

Table 3.5 BET Surface Areas of Uncoated γ-Fe_2O_3 Nanoparticles and Allylamine Plasma Polymerized γ-Fe_2O_3 Nanoparticles

Samples	BET Surface Area (m^2/g)
Uncoated γ-Fe_2O_3	51.8
Allylamine Coated γ-Fe_2O_3, A (10/100ms, 200W, 30min)	44.2
Allylamine Coated γ-Fe_2O_3, B (10/40ms, 200W, 30min)	43.9

In this work, a simple surface modification method ---- pulsed plasma polymerization process was developed to functionalize γ-Fe_2O_3 nanoparticles with free amine groups using the monomer allylamine. The experimental studies showed that pulsed plasma polymerization process not only can functionalize nanoparticle surfaces, but also can improve nanoparticle dispersion. HRTEM images indicated that polyallylamine film was uniformly deposited on the surfaces of γ-Fe_2O_3 nanoparticles

with an average thickness of 4 nm. FTIR, XPS, and ToF-SIMS studies confirmed the presence of polyallylamine. Polyallylamine film on the surfaces of γ-Fe_2O_3 nanoparticles provides an opportunity to immobilize foreign molecules, so that γ-Fe_2O_3 nanoparticles could be utilized as potential drug carriers in the biochemical environment.

3.4 Pulsed Plasma Polymerization of 1,1,1-Trichloroethane

In this work, the effect of plasma peak power input, duty cycles and coating temperatures on the polymer compositions obtained from 1,1,1-trichloroethane (111-TCE) by pulsed plasma polymerization was examined. This is the first study of the plasma polymerization of 1,1,1-trichloroethane. A long range objective of this work is development of films having relatively high Cl atom content for use in a variety of applications.

The variations in film compositions, with variations in duty cycles, were observed for polymers obtained during plasma polymerization of 111-TCE monomer. These variations were revealed by XPS and FTIR spectral analysis of these polymers. FTIR spectra of the films obtained from pulsed plasma 111-TCE films at a peak power of 100W with duty cycles ranging from 10/25 to 10/500 ms are shown in Figure 3.17. The presence of C=C groups in these films is shown by the absorption bands at ~1631 cm^{-1} (C=C stretching) and 3020-3080 cm^{-1} (C=C-H stretching). The relative intensity of C-Cl stretching band at 754 cm^{-1} decreased with increased plasma off time, indicating that the retention of chlorine is reduced with increasing off time. This result is also confirmed by XPS analysis of these polymers. The Cl/C atomic ratios in plasma deposited 111-TCE films are provided in Table 3.6. The Cl/C ratios are shown for both atom percentages obtained from the integrated atom scans and for those calculated from the deconvoluted

high resolution C (1s) peaks. The C(1s) high resolution spectra were deconvoluted into five peaks: $\underline{C}Cl_3$ (288.50eV), $\underline{C}Cl_2$ (287.63eV), $\underline{C}Cl$-CCl (286.44eV), $\underline{C}Cl$ (285.70eV), $\underline{C}$-C (284.90eV), as shown in Figure 3.18. The C(1s) peak assignments are made in light of

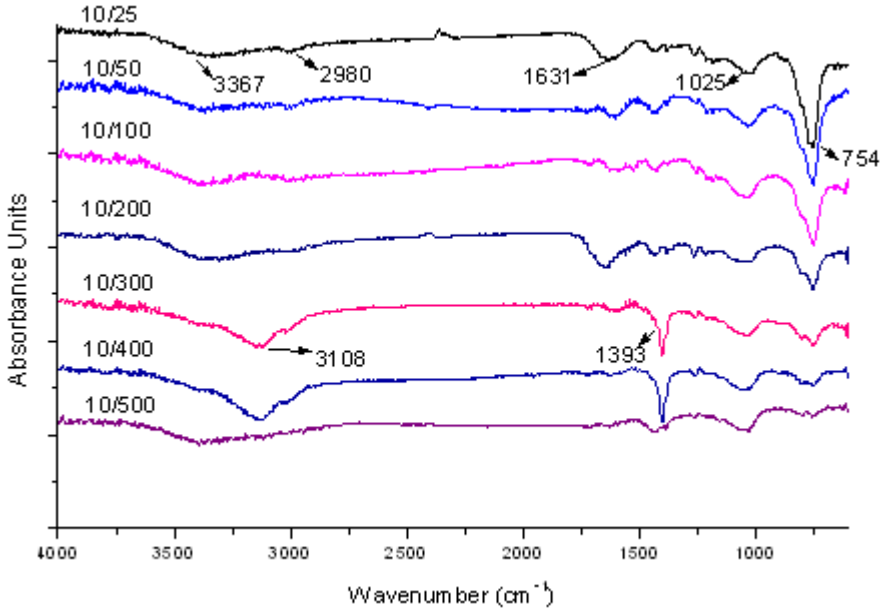

Fig. 3.17 FTIR spectra of pulsed plasma 111-TCE films at a peak power of 100W with duty cycles ranging from 10/25 to 10/500 ms

Table 3.6 Cl/C Atomic Ratios in Plasma Deposited 111-TCE Films Comparing Values Obtained Directly from High Resolution Cl(2p) and C(1s) Spectra to Those Calculated from the Deconvoluted C(1s) Multiplets Spectra

RF Duty Cycle (on/off, ms)	Relative Concentration (%)					Cl/C Ratio	
	$\underline{C}$-Cl_3	$\underline{C}$-Cl_2	$\underline{C}Cl$-CCl	$\underline{C}$-Cl	$\underline{C}$-C	Observed Directly From XPS	Calculated From C(1s) Multiplets
	288.50	287.63	286.44	285.70	284.9		
10/25	5.97	20.25	19.95	31.96	21.87	1.08	1.10
10/50	4.88	17.39	21.37	29.38	26.98	1.00	1.00
10/100	7.00	13.77	28.32	29.08	21.84	1.05	1.06
10/200	5.38	14.80	21.55	27.89	30.39	0.95	0.95
10/300	5.96	12.72	21.42	27.42	32.49	0.93	0.92
10/400	5.31	11.63	23.82	26.50	32.75	0.92	0.90
10/500	5.41	11.29	24.01	26.32	32.97	0.92	0.90

those reported by Chen in a study of the $CHCl_3$. [49]Good agreement is obtained between these two analysis, as shown in Table 3.6. Overall, a decrease in Cl/C film atom ratios from 1.08 to 0.92 is obtained with increasing plasma off time from 25 ms to 500ms. The increased elimination of Cl atoms with decreasing plasma duty cycle is an interesting result in that this is contrary to the generally observed trend of increased retention of monomer functional groups in plasma polymers as the average power input is decreased.

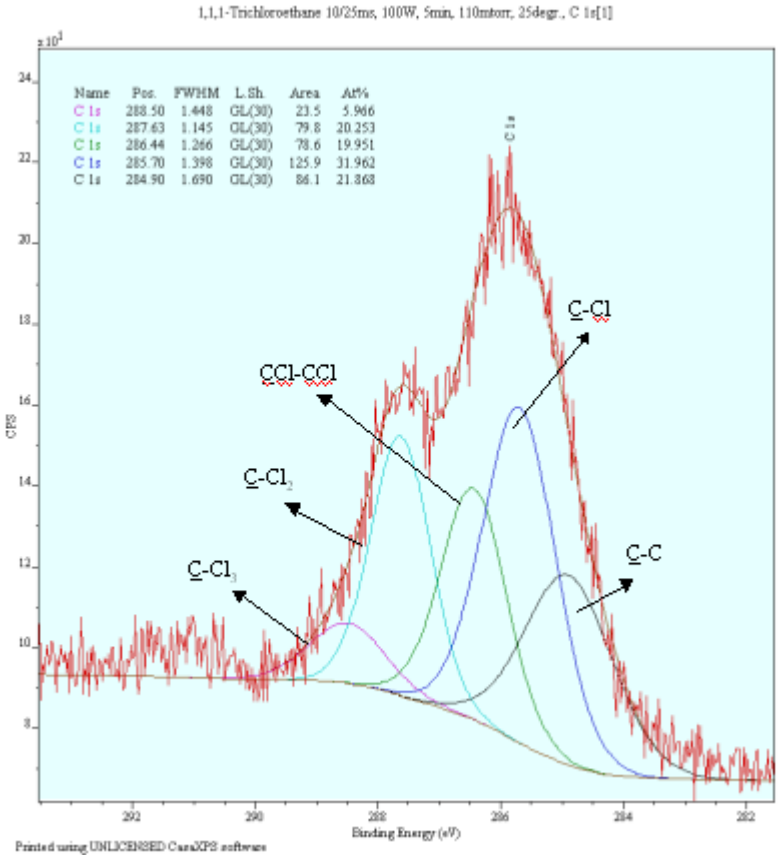

Fig. 3.18 High resolution C(1s) XPS spectrum of pulsed plasma polymerized 1,1,1-trichloroethane film at a duty cycle of 10/25ms and a peak power of 100W

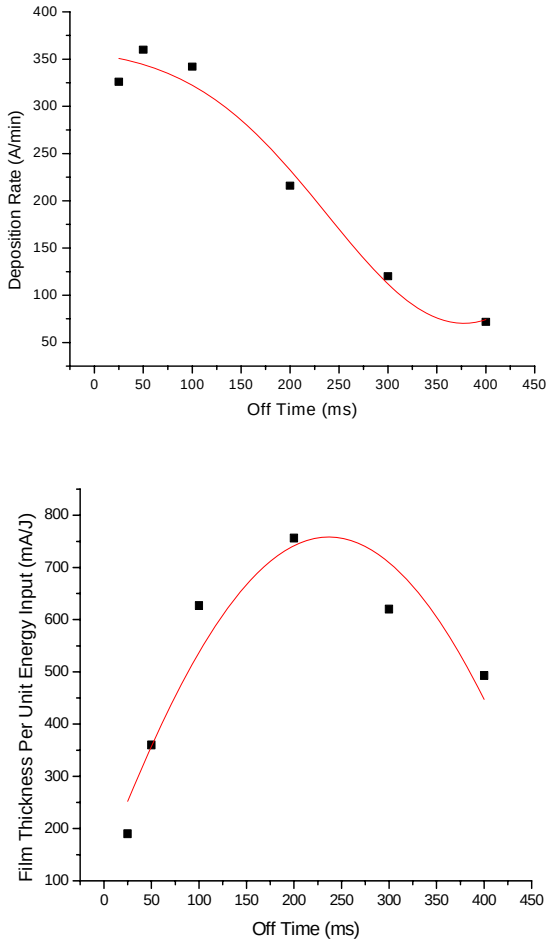

Fig. 3.19 Variation in deposition rate and thickness per unit energy input as a function of plasma off time for pulsed plasma polymerized 111-TCE films obtained at constant plasma on time of 10 ms and peak power of 100W

Deposition rate and film thickness per unit energy input data, derived from profilometer measurements of plasma polymerized 111-TCE films deposited on polished silicon substrates at constant plasma on time of 10ms and peak power of 100W, are shown in Figure 3.19. The film deposition rates (Å/min) decreased, in general, with the increasing off time (with decreased average power). However, the energy efficiency plot of film formation illustrates an initial increase in film thickness growth per unit energy input with increasing off time reaching a maximum for 250ms off time run. At longer

plasma off times, the energy efficiency begins to decrease. The increasing film thickness per unit energy input with initial decreasing average power input is evidence for film formation during plasma off times. The decrease in film formation energy efficiency observed for longer plasma off times, may reflect complete scavenging of all radical intermediates during the long off times leading to subsequent poor coupling of efficient power input into the reactor under these conditions.

The variations in film compositions with variations in peak power inputs were also studied for polymers obtained during plasma polymerization of 111-TCE monomer. These variations were revealed by XPS and FTIR spectral analysis of these polymers. The film chemistry of pulsed plasma deposited films from 111-TCE varies with changes in the RF peak power input employed. FTIR spectra of the films obtained at a fixed duty cycle of 10/25 ms with peak power input ranging from 10W to 200W are shown in Figure 3.20. IR absorption bands at 2980 cm^{-1} (C-H stretching), 1432 $cm^{-1}$and 1393 cm^{-1} (C-H bending) are characteristic bands of hydrocarbon groups. Retention of Cl atoms in the polymer films is confirmed by the absorption band at 755 cm^{-1} (C-Cl stretching). The presence of C=C groups in these films is indicated by IR absorption bands at ~1627 cm^{-1} (C=C stretching) and 3020-3080 cm^{-1} (C=C-H stretching). The relative intensity of this C=C stretching band increases slightly with increased plasma peak power input, consistent with increased dehydrogenation and/or dehydrohalogenation processes at higher power inputs.

As before, the XPS C(1s) high resolution spectra were deconvoluted into five peaks: $\underline{C}Cl_3$ (288.15eV), $\underline{C}Cl_2$ (287.66eV), $\underline{C}$Cl-CCl (286.51eV), $\underline{C}$Cl (286.04eV), $\underline{C}$-C (284.90eV). The Cl/C atomic ratios in plasma deposited 111-TCE films, comparing

values obtained directly from high resolution Cl(2p) and C(1s) spectra to those calculated from the deconvoluted C(1s) multiplet spectra at a fixed duty cycle of 10/25 ms with peak power ranging from 10W to 200W, are shown in Table 3.7. Again, excellent agreement is obtained between these two sets of values.

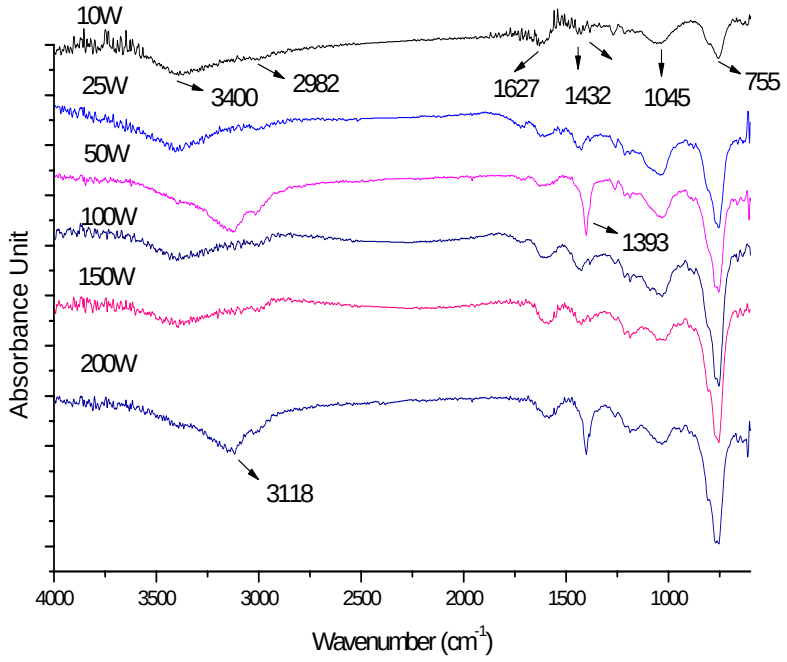

Fig. 3.20 FTIR spectra of pulsed plasma 111-TCE films at a duty cycle of 10/25 ms with peak powers ranging from 10 to 200 W

As shown in Table 3.7, the Cl/C ratios illustrate an initial increase from 0.99 to 1.11 when the peak power increases from 10W to 50W; then it drops to 0.97 when the peak power goes up to 200W. The initial increased Cl retention with increasing power input is consistent with the previously noted Cl/C variations with changing plasma duty cycle (increased Cl/C ratio with increasing average power input). The subsequent decrease in Cl/C ratios at even higher power inputs most probably arises from the

increased importance of surface ablation processes in which breakage of the relatively weak C-Cl bonds occur preferentially.

Deposition rate and thickness per unit energy input data, derived from plasma polymerized 111-TCE films deposited on polished silicon substrates at a fixed plasma duty cycle of 10/25 ms and peak power from 10 to 200W, are shown in Figure 3.21. The film deposition rates (Å/min) increase, in general, with the increasing peak power (increasing average power). However, the energy efficiency plot of film formation indicates a decrease with increasing peak power. This latter result is consistent with an increased occurrence of ablation processes with increasing power inputs, as noted above.

Table 3.7 Cl/C Atomic Ratios in Plasma Deposited 111-TCE Films Comparing Values Obtained Directly from High Resolution Cl(2p) and C(1s) Spectra to Those Calculated from the Deconvoluted C(1s) Multiplet Spectra at a Fixed Duty Cycle of 10/25 with Peak Power Ranging from 10 W to 200W

Peak Power (W)	Relative Concentrations (%)					Cl/C ratio	
	$\underline{C}$-Cl_3	$\underline{C}$-Cl_2	$\underline{C}Cl$-$\underline{C}Cl$	$\underline{C}$-Cl	$\underline{C}$-C	Observed Directly Form XPS	Calculated From C(1s) Multiplets
	288.15	287.66	286.51	286.04	284.9		
10	4.95	15.64	29.30	22.03	28.09	0.99	0.97
25	4.91	18.22	21.23	33.53	22.11	1.08	1.06
50	5.61	19.28	20.70	32.94	21.41	1.11	1.10
100	5.63	17.42	22.53	28.84	25.58	1.04	1.03
150	5.39	14.82	28.81	23.56	27.42	0.99	0.98
200	4.06	14.02	33.33	23.68	24.91	0.97	0.97

.

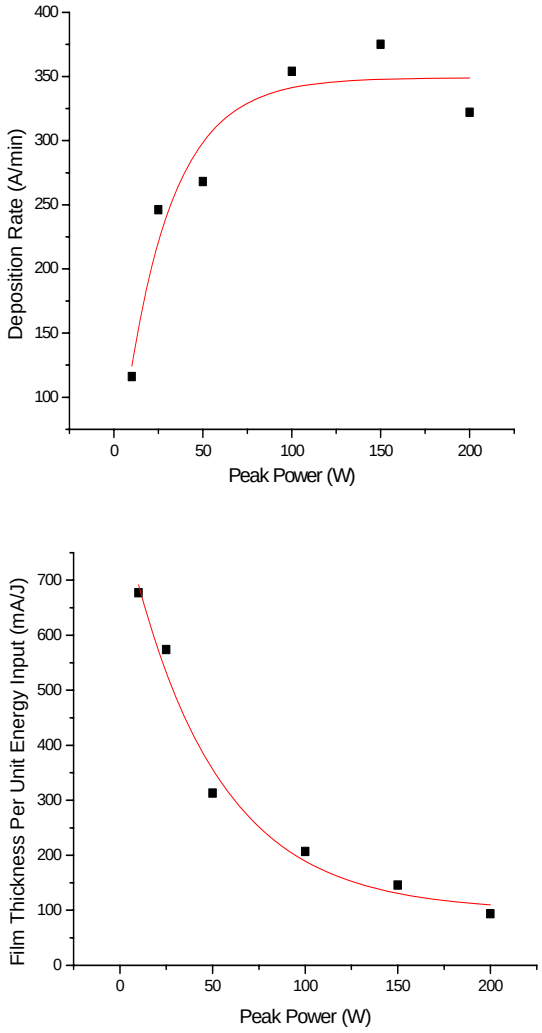

Fig. 3.21 Variation in film deposition rate and thickness per unit energy input as a function of plasma peak power for pulsed plasma polymerized 111-TCE films obtained at a constant plasma duty cycle 10/25 ms

The film composition obtained from pulsed plasma polymerization of 111-TCE as a function of substrate temperatures was also investigated. FTIR spectra of the films at substrate temperatures ranging from 25 to 100°C, all deposited at a 10/25 ms duty cycle and 100W power input, are shown in Figure 3.22. Inspections of these spectra reveal essentially no film compositional changes with variations in substrate temperatures. This result was confirmed with XPS analysis (Table 3.8), which revealed essentially little

variation in Cl/ C atom ratios with substrate temperatures variation. The small variation in Cl/C ratios indicates less Cl atom retention in the polymer film with increasing substrate temperature. Again, this result would be consistent with increased surface ablation with increasing reaction temperature. Both film deposition rate and energy efficiency plots (thickness per unit energy input) (Fig. 3.23) were observed to decrease with increased coating temperature, which would be consistent with increased ablation reaction.

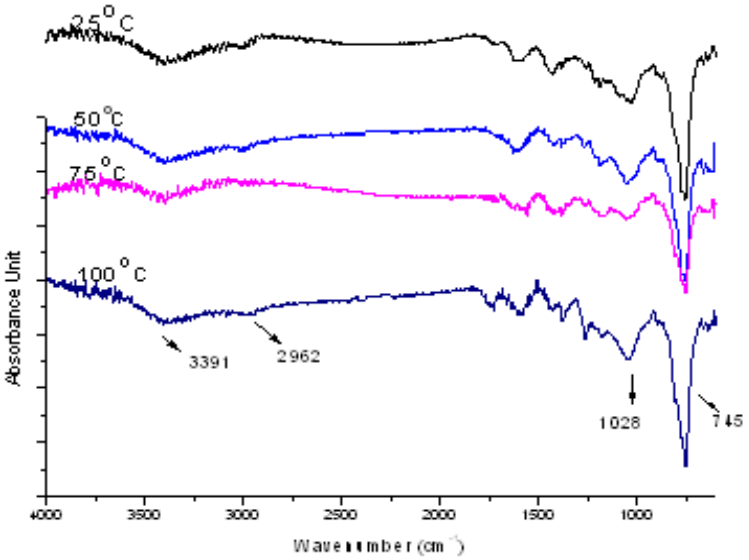

Fig. 3.22 FTIR spectra of pulsed plasma 111-TCE films at a duty cycle of 10/25 ms and a peak power of 100 W with temperatures ranging from 25°C to 100 °C

Table 3.8 Cl/C Atomic Ratios in Plasma Deposited 111-TCE Films Comparing Values Obtained Directly from High Resolution Cl(2p) and C(1s) Spectra to Those Calculated from the Deconvoluted C(1s) Multiplet Spectra at a Peak Power of 100W and Duty Cycle of 10/25ms with Different Coating Temperatures

Coating Temperature (°C)	Relative Concentration (%)					Cl/C ratio	
	<u>C</u>-Cl_3	<u>C</u>-Cl_2	<u>C</u>Cl-C<u>C</u>l	<u>C</u>-Cl	<u>C</u>-C	Observed Directly From XPS	Calculated From C(1s) Multiplets
	288.42	287,66	286.30	285.77	284.90		
25	5.97	20.25	19.95	31.96	21.87	1.08	1.10
50	5.64	17.96	18.78	29.35	21.49	1.00	1.01
75	4.54	16.08	27.66	27.87	23.85	1.01	1.01
118	4.30	12.58	22.75	37.39	22.99	0.98	0.98

In this work, the effects of plasma duty cycle, plasma peak power input and coating temperature on the controllability and variation in the film chemistry of polymer films obtained under pulsed plasma polymerization of 1,1,1-trichloroethane was examined. Although film chemistry variations were observed, the magnitude of such variations in terms of changes in atom ratios was less than that observed for other monomers. Surprisingly, the amount of chlorine retained in the polymer films decreased as the average power input during polymerization was decreased. In other monomers studied to date, the heteroatom atom content of the polymers increased as the average power input is decreased. In the present case, the unexpected result might arise from enhanced molecular eliminations as the power input, and thus electron energies in the discharge are reduced. For example, molecular elimination of HCl would be an energetically favorable process. The presence of C=C bonds in the polymer films can be cited in support of this molecular elimination route.

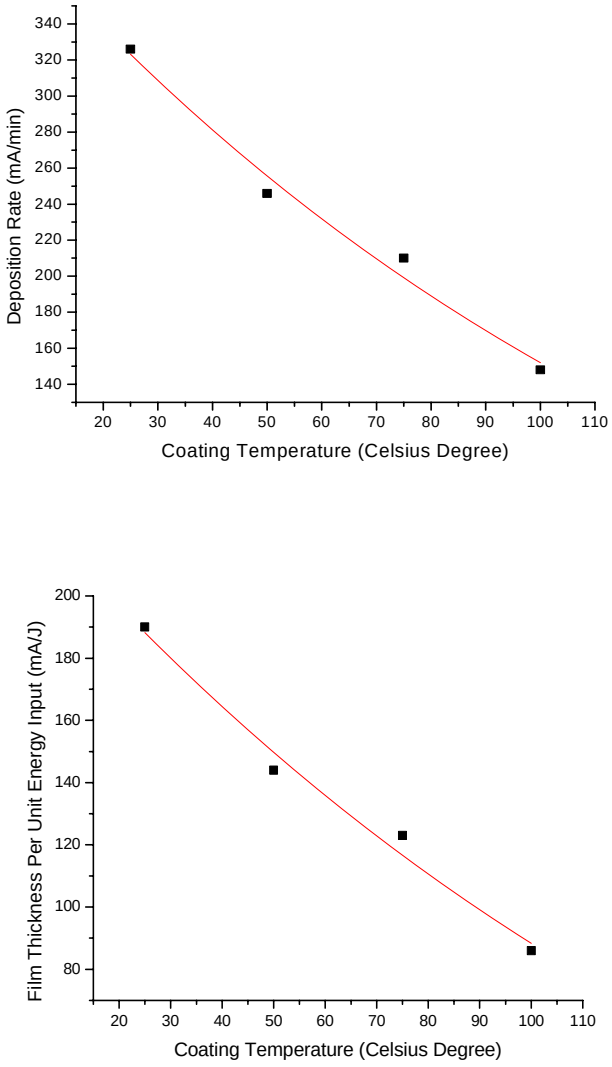

Fig. 3.23 Variation in film deposition rate and thickness per unit energy input as a function of coating temperature for pulsed plasma polymerized 111-TCE films obtained at a constant duty cycle of 10/25 ms and peak power of 100W

CHAPTER 4

SUMMARY

The objectives of this study, surface functionalization of polymer substrates and nanoparticles via pulsed plasma polymerization process, have been met with a variety of starting monomers and various substrates. The starting monomers include maleic anhydride, glycidyl methacrylate, citraconic acid, 1,1,1-trichloroethane, ethylenediamine and allylamine. The surface functionalizations have been operated on PEEK polymer substrates and γ-Fe_2O_3 nanoparticles. With each of these monomers, the film chemistry controllability was achieved by varying the RF duty cycles employed during the film deposition process, all other variables being held constant.

The major observations and conclusions for each study in this work can be summarized as follows:

1. A solventless ultra-thin film process was developed successfully to bond polymeric substrates. A strong adhesive bonding was obtained between two PEEK substrates using polymers generated from the pulsed plasma polymerization of glycidyl methacrylate and allylamine. Glycidyl methacrylate and allylamine were plasma polymerized individually on two PEEK substrates. However, the strongest bonding achieved between the two PEEK surfaces was from the pulsed plasma polymerization of the mixture of glycidyl methacrylate and methacrylic acid (3:1) using ethylenediamine as a coupling agent.

2. The second part of this thesis represents the first examination of the plasma polymerization of a dicarboxylic acid, namely, citraconic acid. In the pulsed plasma polymerization of citraconic acid, systematically decreasing plasma RF duty cycles resulted in enhanced -COOH retention in the resultant films. This result is consistent with formation of more highly cross-linked polymeric film as the power input is increased. But the relatively low overall retention of carboxylic group, coupled with the low volatility of the monomer, make citraconic acid not a good candidate for the purpose of creating polymeric thin film coatings having a high concentration of –COOH groups.

3. The third part of this thesis introduced the use of pulsed plasma polymerizations to functionalize γ-Fe_2O_3 nanoparticles. In the present case, this capability was demonstrated using plasma polymerization of allylamine monomer. The experimental studies showed that pulsed plasma polymerization process not only can functionalize nanoparticle surfaces, but also can improve nanoparticle dispersion. HRTEM images indicated that polyallylamine film could be uniformly deposited on the surfaces of γ-Fe_2O_3 nanoparticles. FTIR, XPS, ToF-SIMS have confirmed the presence of polyallylamine on these nanoparticles.

4. The fourth part of this thesis is the pulsed plasma polymerization of 1,1,1-trichloroethane. The effects of plasma duty cycle, plasma peak power input and coating temperature on the controllability and variation in the film chemistry of polymer films were investigated. The amount of chlorine retained in the polymer films decreased as the average power input during polymerization is decreased. This unexpected result might arise from enhanced molecular eliminations as the power input and thus electron energies in the discharge are reduced.

REFERENCES

(1) Yasuda, H., Plasma Polymerization, Academic Press, New York, 1996

(2) Chapman, B. N., Glow Discharge Processes: Sputtering and Plasma Etching, John Wiley & Sons, Inc., New York, 1980

(3) (a)Rinsch, C. L., Chen, X., Panchalingam, V., Eberhart, R. C., Wang, J. H.,Timmons, R. B., Langmuir, 12, 2995, 1996

(b) Wang J. H., Chen, J. J., R. B. Timmons, Chemistry of Materials, 8, 2212, 1996

(c) Chen, X., Rajeshwar, K., Timmons, R. B., Chen, J. J., Chyan, O. M. R., Chemistry of Materials, 8, 1067, 1996

(d) Han L. C., Rajeshwar, K., Timmons, R. B., Langmuir, 13 (2), 5941, 1997

(e) Tang, L., Wu, Y., Timmons, R. B., Journal of Biomedical Material Research, 42 (1), 156, 1998

(4) M. A. Burns al., Science 282, 484, 1998

(5) H. P. Chou. Spence, A. Scherer, S. R. Quake, Proc. Natl. Acad. Sci. U. S. A. 96, 11, 1999

(6) D. A. Dunn, I. Feygin, Drug Discovery Today, 5, S84, 2000

(7) M. W. Losey, M. A. Schmidt, K. F. Jensen, Industrial and Engineering Chemistry Research, 40, 2555, 2001

(8) T. S. Sammarco, Mark A. Burns, Journal of Micromechanics and Microengineering, 10, 42-55, 2000

(9) C. M. Matzke, C. I. H. Ashby, et., U. S. Patent, 6,096,656, Aug. 1st, 2000

(10) A. J. Kinloch, Durability of Structural Adhesive, London & New York

(11) N. V. Bhat, D. J. Upadhyay, Journal of Applied Polymer Science, 86, 925-936, 2002

(12) A. Nihlstraud, T. Hjertberg, K. Johanson, Polymer, Vol. 38, No. 7, 1557, 1997

(13) J. Krudi, H. Ardelean, P. Marcus, et. Applied Surface Science, 189, 119-128, 2002

(14) L. J. Gerenser, Journal of Vacuum Science and Technology, A 6(5), Sep/Oct, 2897-2903, 1988

(15) M. Mori, Y. Uyama, et. Journal of Polymer Science, Part A: Polymer Chemistry, 32, 1683, 1994

(16) S. L. Kaplan, E. S. Lopata and J. Smith, Surface and Interface Analysis, 20, 331, 1993

(17) X. P. Zou, E. T. Kang, K. G. Neoh, C. Q. Cui, T. B. Lim, Polymer, 42, 6409, 2001

(18) X. P. Zou, E. T. Kang, et. Plasma and Polymer, Vol. 5, No. 5, ¾, 2000

(19) M. Morra, E. Occhiello and F. Garbassi, Surface and Interface Analysis, 16, 412, 1990

(20) S. A. Evenson, C. A. Fail and J. P. S. Badyal, Chemistry of Materials, 12, 3038, 2000

(a) G. H. Yang, E. T. Kang, K. G. Neoh, Journal of Polymer Science, Part A: Polymer Chemistry, Vol. 38, 3498, 2000

(21) C. Tarducci, W. C. E. Schofield, and J. P. Badyal, Chemistry of Materials, 14 (6), 2541, 2002

(22) L.M. Han, R. B. Timmons, Journal of Polymer Science Part A: Polymer Chemistry, Vol. 36, No. 17, 3121, 1998

(23) A. P. Kettle, A. J. Beck, L. O'Toole, F. R. Jones, R. D. Short, Composites Science and Technology, 57 (8), 1023, 1997

(24) D. L. Cho, O. J. Ekengren, Journal of Applied Polymer Science, 47, 1601, 1993

(25) V. N. Vasilets, G. Hermel, U. Konig, C. Werner, M. Muller, F. Simon, K. Grundke, Y. Ikada, H. J. Jacobsch, Biomaterials, 18, 1139, 1997

(26) T. M. Ko, J. C. Lin, S. L. Cooper, Journal of Colloid and Interface Science, 156, 207, 1993

(27) L. O'Toole, A. J. Beck, R. D. Short, Macromolecules, 29, 5172, 1996

(28) D. K. Kim, Y. Zhang, W. Voit, K. V. Rao, J. Kehr, B. Bjelke and M. Muhammed, Scripta Materialia, 44, 1713, 2001

(29) L. Babes, B. Dennizot, G. Tanguy, J. J. Le Jeune, P. Jallet, Journal of Colloid and Interface Science, 212, 474, 1999

(30) M. I. Papisov, A. Bogdanov Jr., B. Schaffer, N. Nossiff, T. Shen, R. Weissleder, T. J. Brady, Journal of Magnetism and Magnetic Materials, 122,383, 1993

(31) N. Nitin, L. E, W, LaConte, O. Zurkiya, X. Hu, Journal of Biological Inorganic Chemistry, 9, 706, 2004

(32) S. Roath, Journal of Magnetism and Magnetic Materials, 122, 329, 1993

(33) A. Jordan, R. Scholz, P. Wust, H. Schirra, T. Schiestel, H. Schmidt, R. Felix, Journal of Magnetism and Magnetic Materials, 194, 185, 1999

(34) A. K. Gupta, A. S. G. Curtis, Journal of Materials Science: Materials in Medicine, 15, 493, 2004

(35) S. R. Rudge, T. L. Kurtz, C. R. Vessely, L. G. Catterall, D. L. Williamson, Biomaterials, 21, 1411, 2000

(36) P. K. Gupta, C. T. Hung, Life Sciences, 44, 175, 1989

(37) C. Bergemann, D. Müller-Schulte, J. Oster, L. à Brassard, A. S. Lübbe, Journal of Magnetism and Magnetic Materials, 194, 45, 1999

(38) H. Gu, P. Ho, K. W. T. Tsang, L. Wang, B. Xu, Journal of the American Chemical Society, 125, 15702, 2003

(39) S. Yu, G. M. Chow, Journal of Materials Chemistry, 14, 2781, 2004

(40) L. A. Harris, J. D. Goff, A. Y. Carmichael, J. S. Riffle, J. J. Harburn, T. G. St. Pierre, M. Saunders, Chemistry of Materials, 15, 1367, 2003

(41) C.Xu, K. Xu, H. Gu, R. Zheng, H. Liu, X. Zhang, Z. Guo, B. Xu, Journal of the American Chemical Society, 126, 9938, 2004

(42) M. Mikhaylova, D. K. Kim, C. C. Berry, A. Zagorodni, M.Toprak, A. S. G. Curtis, M. Muhammed, Chemistry of Materials, 16, 2344, 2004

(43) M. Ma, Y. Zhang, W. Yu, H. Shen, H. Zhang, N. Gu, Colloids and Surfaces A: Physicochemical Engineer Aspects, 212, 219, 2003

(44) B. Yoza, M. Matsumoto, T. Matsunaga, Journal of Biotechnology, 94, 217, 2002

(45) L. O'Toole, A. J. Beck, R. D. Short, Macromolecules, 29, 5172, 1996

(46) George Socrates, Infrared Characteristic Group Frequencies: Table and Charts, (second edition) John Wiley & Sons, 1994

(47) P.Tartaj, M. P. Morales, S. Veintemillas-Verdaguer, T. González-Carreño and C. J. Serna, Journal of Physics, D: Applied Physics, R182, 36, 2003

(48) G. Beamson, D.Briggs, High Resolution XPS of Organic Polymers: The Scienta ESCA 300 Database, John Wiley & Sons

(49) Xiaolan Chen, Ph. D dissertation, UT at Arlington

BIOGRAPHICAL INFORMATION

Jing Wu received her Bachelor of Science in Chemistry from Beijing Normal University (Beijing, China) in 1993. She then worked for Xinjiang Institute of Chemistry, Chinese Academy of Sciences from 1993 to 1997 as a research associate in the field of organic synthesis. In 1997, she went to the Graduate School of Chinese Academy of Sciences, and received her Master of Science in Chemistry in 2000. In the summer of 2001, she joined the Department of Chemistry and Biochemistry at the University of Texas at Arlington, and began to work with Professor Richard B. Timmons on RF pulsed plasma polymerization of polymeric thin film materials in 2002.